CHAPTER 4

RESULTS AND DISCUSSION

I SYNTHESIS OF N-(2-PROPYLPENTANOYL) UREA (VPU)

The synthesis of VPU was accomplished by the reaction of 2-propylpentanoyl chloride and urea in dry benzene with the presence of potassium carbonate. The crude VPU synthesized was approximately 50-60% of theoretical yield. The crude product was further purified by recrystallization to yield the first crop of 10-20% theoretical yield. Only the first crop from several lots of synthesis were recrystallized in benzene together to obtained the crystals that will be assigned as a reference form of VPU in future studies to assure the purity and uniformity of crystals.

1.1. Appearance and Morphology

The reference VPU is a white, odorless, needle-like crystal with bulky and static property. The Scanning Electron Microscope (SEM) photomicrographs show the euhedral habit in acicular shape. The crystals, having a size more than 10 μm, have small particles on the surface (Figure 9).

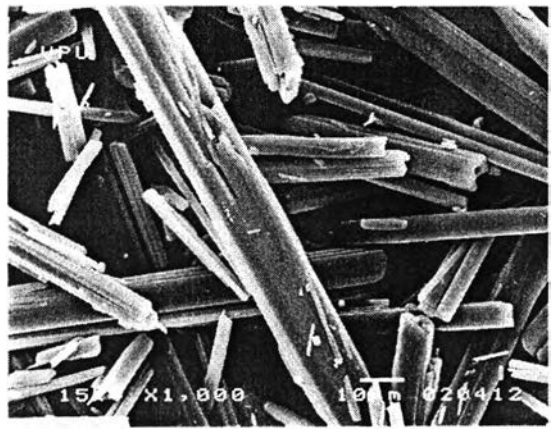

Figure 9: SEM photomicrograph (1000x) of the reference VPU crystals

1.2. Fourier Transform Infrared Spectroscopy

The solid state FTIR was carried out to determine identity of the reference VPU comparing with IR pattern of VPU achieved by Wicharn Janwitayanuchit (5). There were similarities between the FTIR patterns of the reference VPU and the VPU synthesized by Wicharn. The FTIR pattern of the reference VPU shows strong sharp peak at 3400 cm^{-1} for NH stretching vibration of imide, the peak at 3340 cm^{-1} and 3240 cm^{-1} for asymmetric and symmetric NH stretching vibration of primary amide, the strong peak at 1700 cm^{-1} representing C=O stretching vibration (amide I) of imide and the strong peak at 1680 cm^{-1} representing C=O stretching vibration (amide I) of primary amide, the peak at 1590 cm^{-1} representing NH bending vibration (amide II) and the peak at 1355 cm^{-1} for C-N stretching vibration of amide (Figure 10) (5).

1.3. Thin layer chromatography

TLC was used to ensure chemical identity and purity of all VPU samples by comparing with TLC patterns of the VPU samples previously identified by FTIR. TLC was used in this study because of its simplicity, reliability, low cost, and selectivity of detection through the use of various location procedures (59).

The TLC pattern of the reference VPU, using 10 centimeters-long TLC plastic sheet silica gel 60 F_{254} (Merck) and ethyl acetate as a mobile phase, occurred as a single spot at an R_f value of 0.56. The R_f value is calculated by following equation.

$$R_f = \frac{\text{Distance the substance travels from the origin}}{\text{Distance the solvent front travels from the origin}}$$

The spots were located by spraying with Dragendorff reagent which positive for primary amide.

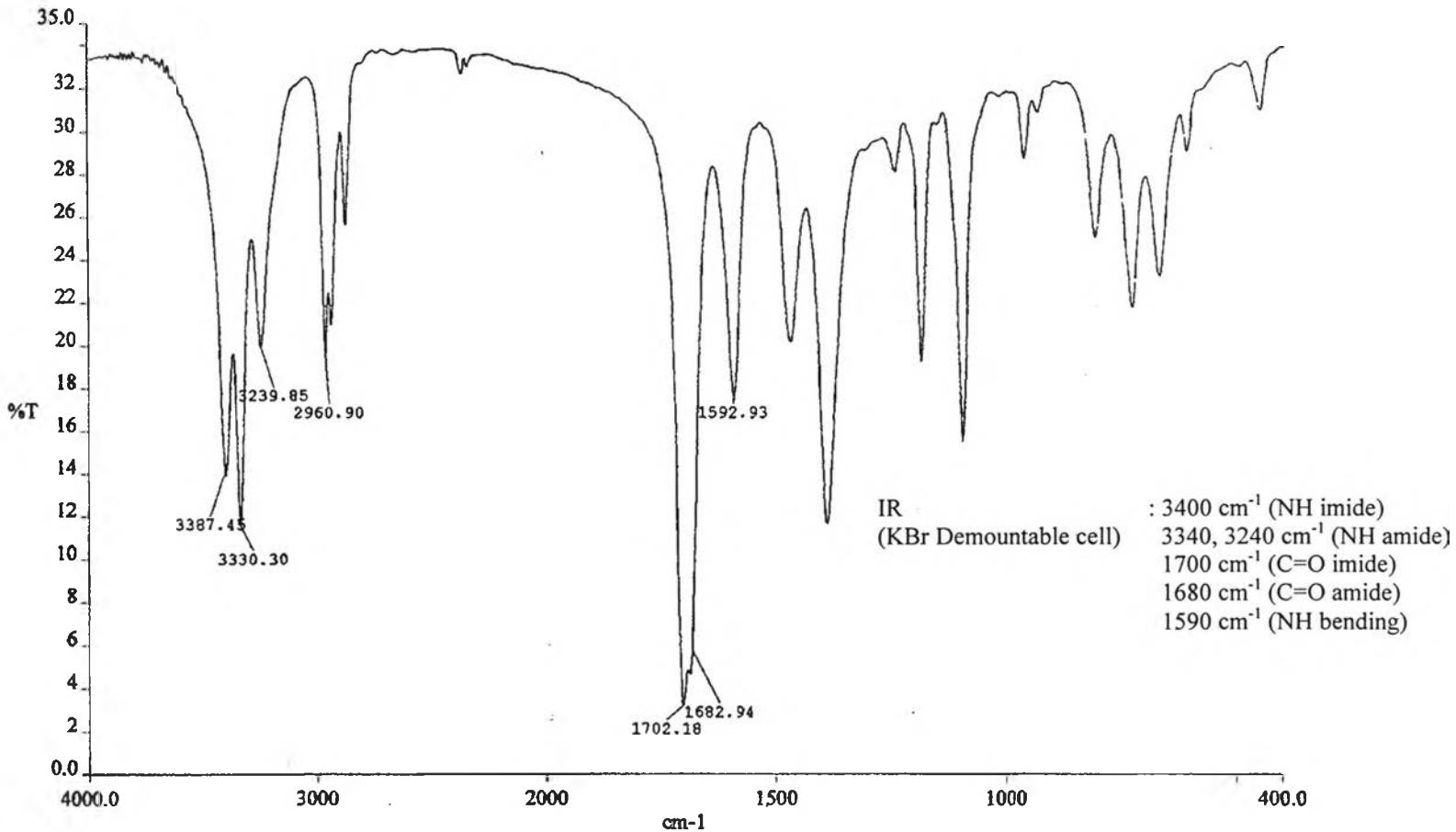

Figure 10: FTIR pattern of the reference VPU

1.4. X-ray Powder Diffraction analysis

X-ray Powder Diffraction (XRPD) pattern of reference VPU exhibits high intensity peaks at 8.4°, 11.2°, 12.2°, 12.9°, 13.4°, 16.7°, 21.0°, 21.6° and 25.2° 2θ as shown in Figure 11.

The peak at 8.4° 2θ is a single peak which exhibits highest intensity and lowest background noise. Thus, it is suitable to use this peak in quantitative analysis in the future study.

1.5. Thermal methods of analysis (DSC and TGA)

Differential scanning calorimetry (DSC) thermogram obtained from the reference VPU at a heating rate of 10°C/min is shown in Figure 12. DSC curve do not show an endothermic peak in the range of 30-150°C, indicating that the crystal was not a solvate or hydrate form. The first DSC endotherm is due to melting at 197°C, while the second peak is possibly due to degradation. The absence of exothermic peak before the second endothermic peak suggested that recrystallization did not occur. Further study by Thermogravimetric Analysis (TGA) together with DSC at a heating rate of 15°C/min (Figure 13) confirmed that there were no weight loss in the range of 30-150°C, suggesting that no solvent was incorporated in the crystal lattice. The rapid weight loss after melting may imply that the second peak of DSC was due to decomposition of VPU which was confirmed by TGA.

The possible decomposed of VPU is the decomposed of urea in VPU molecule. According to one of the decomposition pathway of urea, it spontaneously decomposes to ammonia and biuret at its melting point under atmospheric pressure (75). Thus, VPU at its melting point may decompose similarly. Quench cooling of the melted VPU should be further examined to clarify the decomposed product.

To study the effect of heating rate on DSC thermograms, DSC study was conducted at heating rate of 5° and 10°C/min and DSC/TGA was conducted at a heating rate of 15°C/min. DSC thermograms obtained at heating rates of 5°C/min (Figure 14), 10°C/min (Figure 12) and 15°C/min (Figure 13) were found to be similar. Thus, heating rate of 5°, 10° and 15° C/min did not have a significant impact on the peak temperature of the DSC thermograms of VPU.

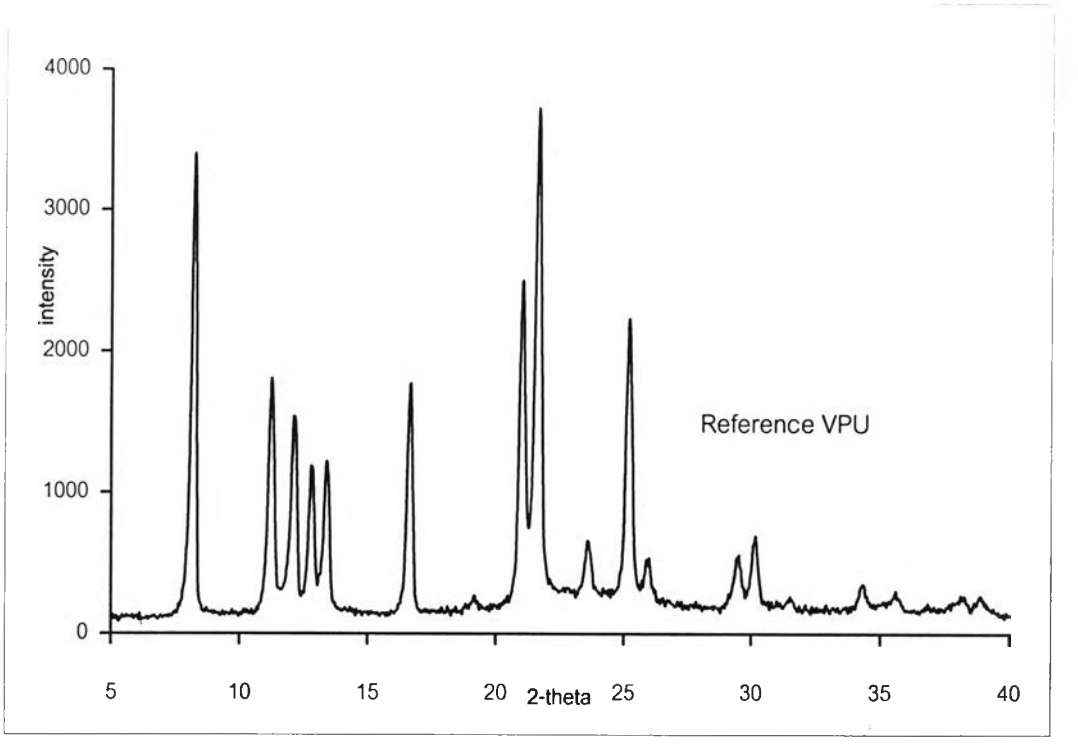

Figure 11: XRPD pattern of the reference VPU

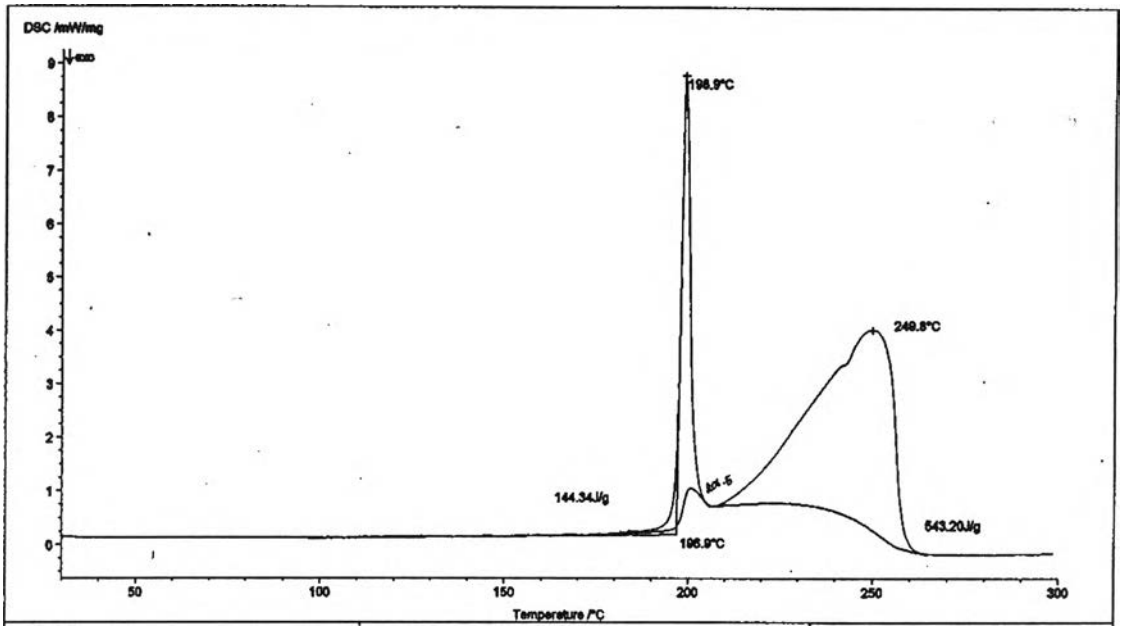

Figure 12: DSC thermogram (10°C/min) obtained from the reference VPU.

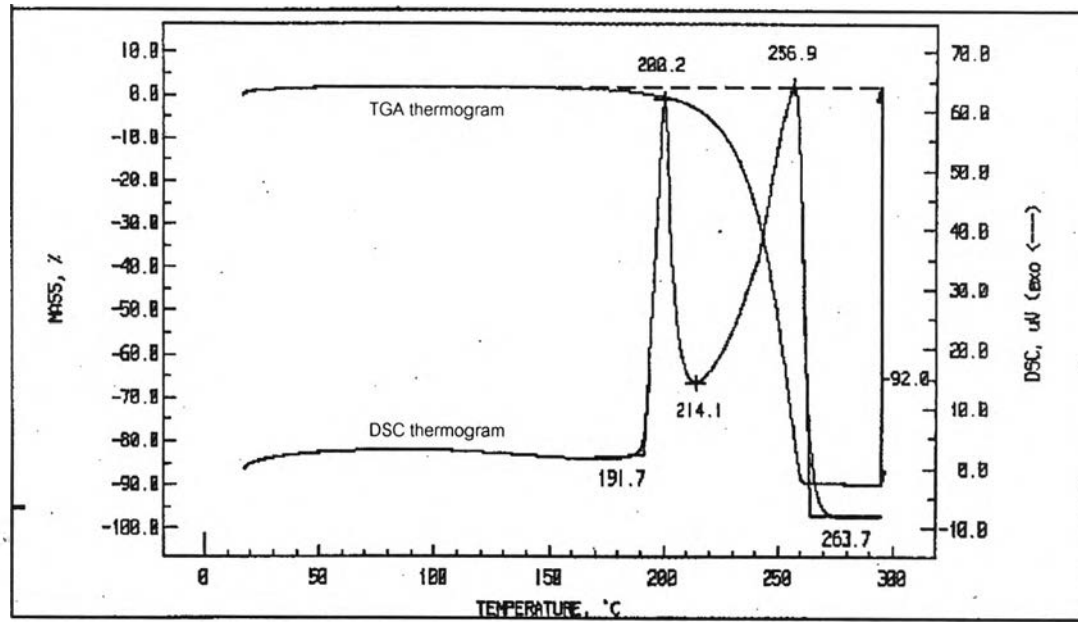

Figure 13: DSC/TGA thermogram (15°C/min) obtained from the reference VPU

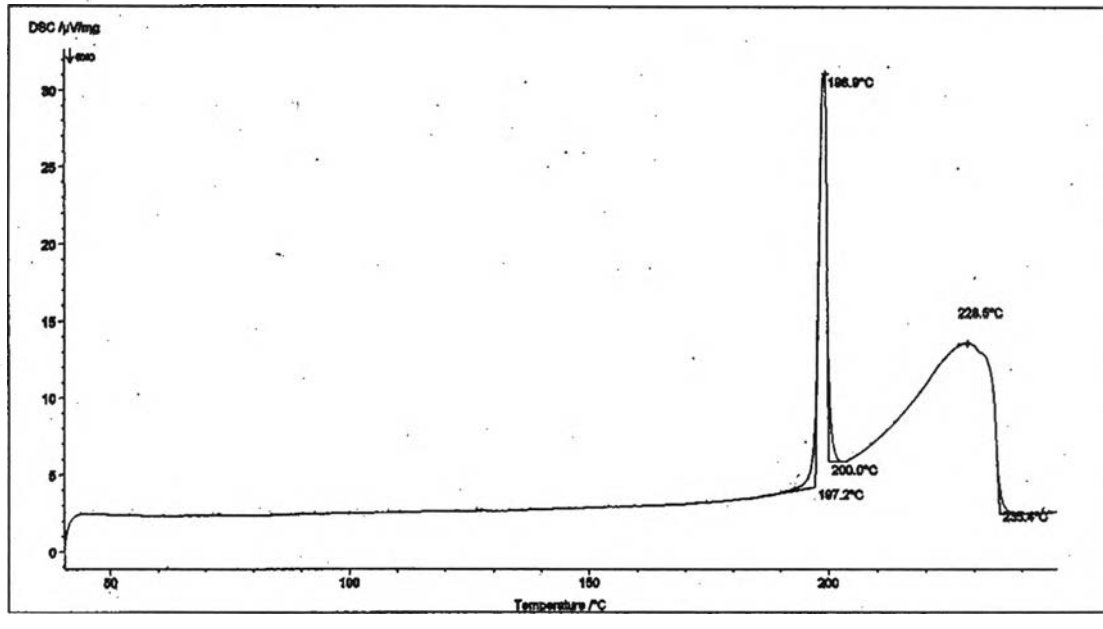

Figure 14: DSC thermogram (5°C/min) obtained from the reference VPU.

II SOLID PHASE SCREENING OF N-(2-PROPYLPENTANOYL) UREA

Attempts were made to treat reference VPU by various techniques in order to obtain its polymorphs, hydrates, solvates or amorphous forms. Since VPU has a poor aqueous solubility property that may prove to be a disadvantage in the future product development. Solid state transformation is one of the opportunity to increase the aqueous solubility of the compound. There are several screening methods for induction of solid phase transformation such as recrystallization in several solvents (methods I-IV), evaporation crystallization (method V), solidification of the melt (method VI) and thermal treatment (method VII).

All of VPU products obtained from various methods mentioned above were identified by TLC and FTIR and then characterized by XRPD. The products tended to have polymorphic or chemical transition based on its XRPD patterns or treating method were selected to examined by TGA and DSC. Morphology of several products were examined by SEM.

2.1. Identification of VPU products

2.1.1 Thin Layer Chromatography

All products were checked for its chemical identity and purity by thin layer chromatography compared with that obtained from the reference VPU. The products obtained from all methods were chemically identical with the reference VPU by occurring in a single spot at the same R_f value (0.56) throughout all the studies. The spots were located by spraying with Dragendorff reagent which positive for primary amide. The R_f values obtained were done under the same condition and calculation methods as previously mentioned.

In addition, to ensure that the degradation products were not occurred, the foreign spots, which may occur, were also detected under ultraviolet light and/or in saturated iodine tank. TLC patterns of the products obtained from all methods did not present any foreign entities. However, TLC is not the high sensitivity analytical method for determination of degradation products. Trace amount of degradation products occurred may not be detectable. Therefore, the decomposition of VPU may occur without detection, especially the products that were heated up to the melting point such as, in our case, the products obtained from evaporation crystallization (method V) and solidification from the melt (VI).

2.1.2 Fourier Transform Infrared Spectroscopy

The products obtained from all methods present the same chemical identity demonstrated by the same FTIR pattern with the reference VPU as shown in Figure 10. The FTIR patterns were also verified with the pattern achieved by Wicharn Janwitayanuchit (5).

2.2. Solid state characterizations of VPU products

2.2.1 Scanning Electron Microscope

Scanning Electron photomicrographs of VPU products at a magnification of 1000X are shown in Figures 15-30.

Morphology of VPU products obtained from recrystallization from various solvents (method I) are needle-like (acicular) form. The products obtained from water and benzene by method II; and acetonitrile, heptane and hexane by method I are long large acicular structure (Figures 15-19). The products obtained from other solvents by method I are presented in short acicular structure with agglomeration (Figures 20-27). This finding may be the result of the degree of supersaturation, as supersaturation is increased, the crystal form tends to change from granular to needle like (12). In method I crystals are obtained by rapid evaporation in this process it may reach supersaturation more quickly and resulted in small acicular structure of crystals (Figures 20-27), while the product recrystallized from water and benzene by method II (Figures 15 and 16) using thermal change may not reach supersaturation as rapidly as method I.

The crystallization solvents having varying polarities also affect crystal structures by forming different types of hydrogen-bonded aggregates, which are related to the crystal structures that developed in the supersaturated solution (48). The study by Etter et al. (49) on crystal structure of acetanilide shows that a hydrogen-bonded chain of molecules is aligned along the needle axis of the crystals. This pattern is characteristic of secondary amides that crystallize in a trans conformation. Hydrophobic solvents such as benzene and carbon tetrachloride will not participate in hydrogen-bond formation, thus the crystals grown by evaporation methods from benzene or carbon tetrachloride are long needles. Solvents that are

proton donors or proton acceptors inhibit chain formation by competing with amide molecules for hydrogen-bonding sites. Thus acetone inhibits chain growth at the –NH end, and methanol inhibits chain growth at the carbonyl end of the chain. Both solvents encourage the formation of rod-like acetanilide crystals, while mixtures of benzene and acetone give hybrid crystals that are rod-shaped, with fine needles growing on the ends.

Since VPU also has secondary amides in its molecule and present needle-like crystal habit as acetanilide, the solvents used in recrystallization may also have the similar effects on VPU crystal. Hydrophobic solvents such as benzene, heptane and hexane may not participate in hydrogen-bond formation, thus the crystals grown from these solvents are long needles. Solvents that are proton donors or proton acceptors such as alcohols, acetone and methylene chloride may inhibit chain formation resulting in short acicular structure.

The products recrystallized from acetone, chloroform, methylene chloride, diethyl ether, ethyl acetate, ethanol, methanol and isopropyl alcohol by method I presented short acicular structure with agglomeration (Figures 20-27). This may result from its small size, which means larger surface area and more electrostatic had occurred. Moreover, all the solvents have low boiling point, which evaporate more rapidly. Thus, VPU supersaturated solution may act as a bridging liquid and deposited on the surface of each small crystals causing it to agglomerate, rather than participating in a complete crystal growth.

The product recrystallized from mixtures of water and ethanol give hybrid crystals that are rod-shaped and needles (Figure 28). The products recrystallized by evaporation crystallization are composed of acicular form and small aggregate that may result from incomplete crystallization (Figure 29). The products obtain from immediate solidification from melts are almost anhedral that may be the result of a very short crystallization time (Figure 30).

However, crystal habit is the result of arrangement of internal structure in the space. Since the internal structure of VPU is unknown, the real arrangement is not predictable. In addition, crystal habit may not only be affected from either hydrogen-bonding or supersaturation of solvent, but it may be resulted from several factors all together.

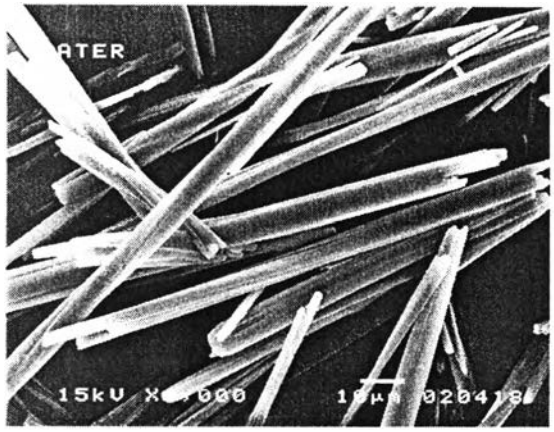

Figure 15: SEM (1000x) of VPU crystal recrystallized from water by method II

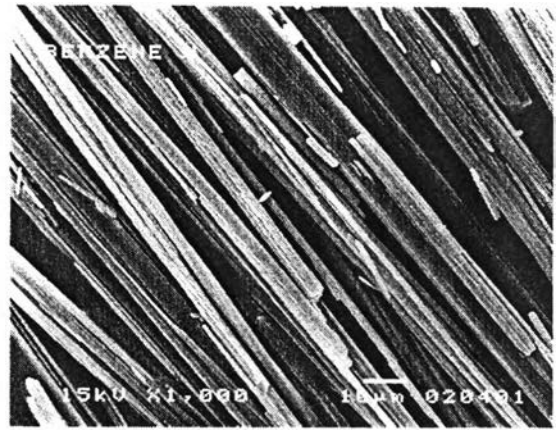

Figure 16: SEM (1000x) of VPU crystal recrystallized from benzene by method II

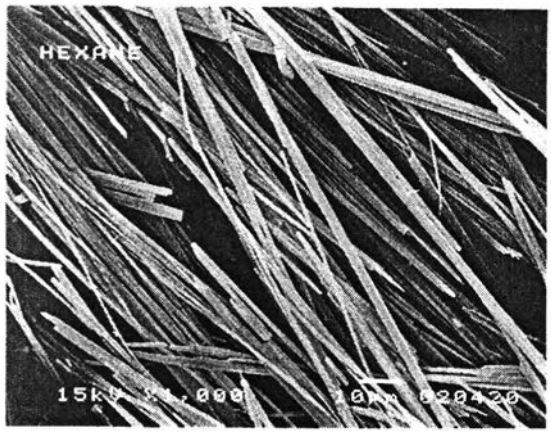

Figure 17: SEM (1000x) of VPU crystal recrystallized from hexane by method I

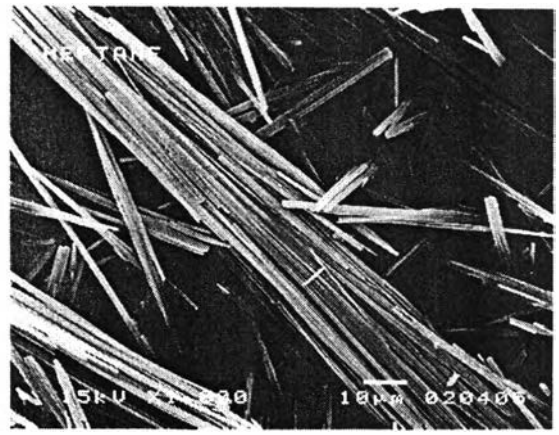

Figure 18: SEM (1000x) of VPU crystal recrystallized from heptane by method I

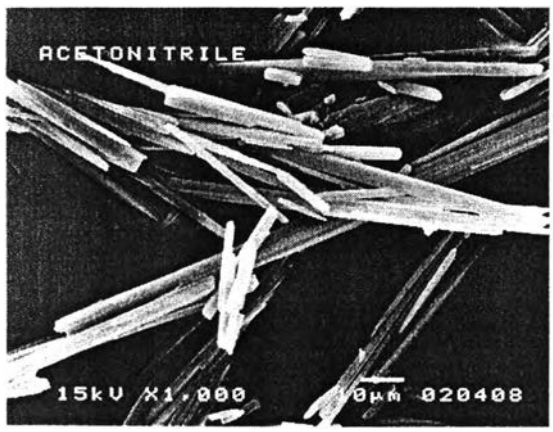

Figure 19: SEM (1000x) of VPU crystal recrystallized from acetonitrile by method I

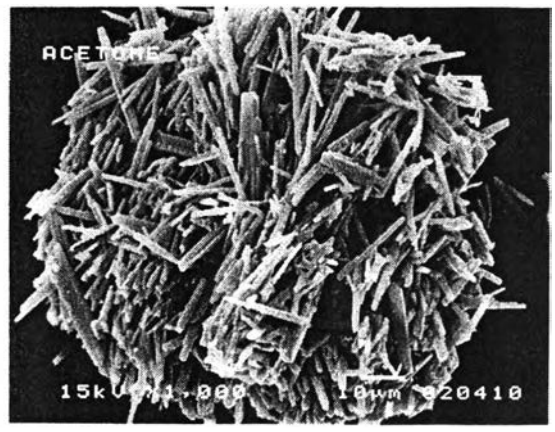

Figure 20: SEM (1000x) of VPU crystal recrystallized from acetone by method I

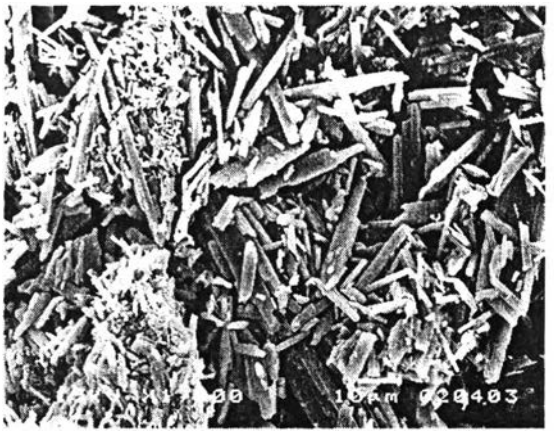

Figure 21: SEM (1000x) of crystal recrystallized from chloroform by method I

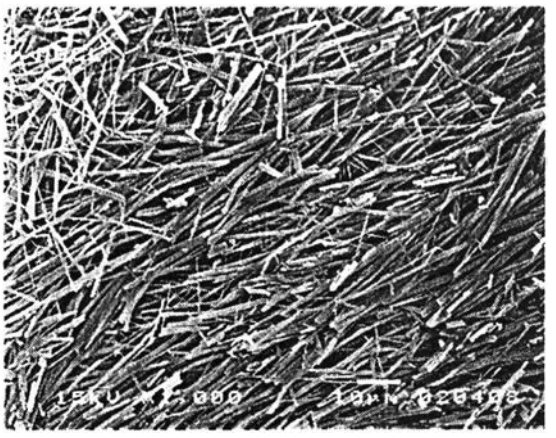

Figure 22: SEM (1000x) of crystal recrystallized from methylene chloride by method I

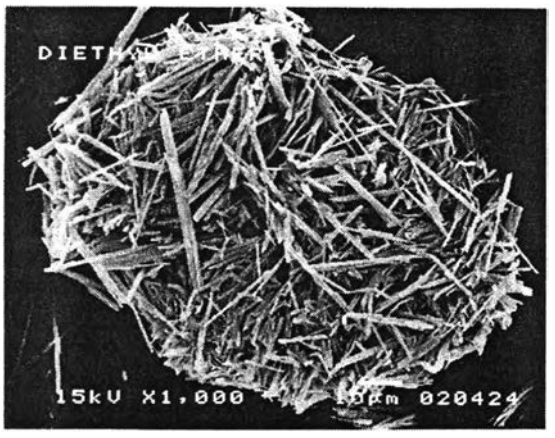

Figure 23: SEM (1000x) of VPU crystal recrystallized from diethyl ether by method I

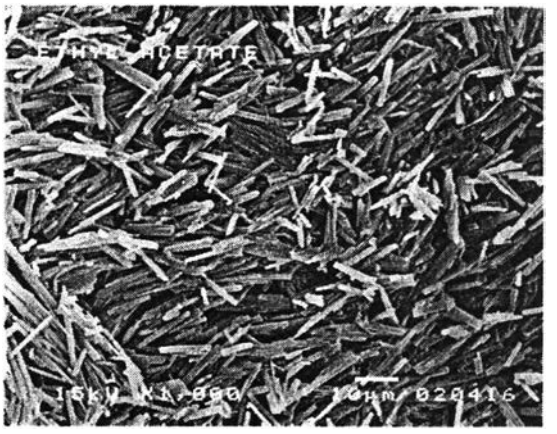

Figure 24: SEM (1000x) of VPU crystal recrystallized from ethyl acetate by method I

Figure 25: SEM (1000x) of VPU crystal recrystallized from ethanol by method I

Figure 26: SEM (1000x) of VPU crystal recrystallized from isopropyl alcohol by method I

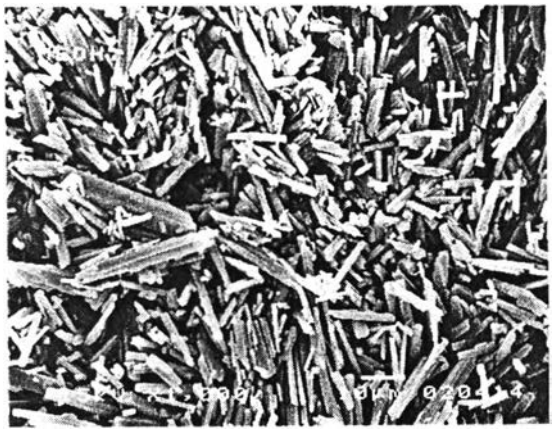

Figure 27: SEM (1000x) of VPU crystal recrystallized from methanol by method I

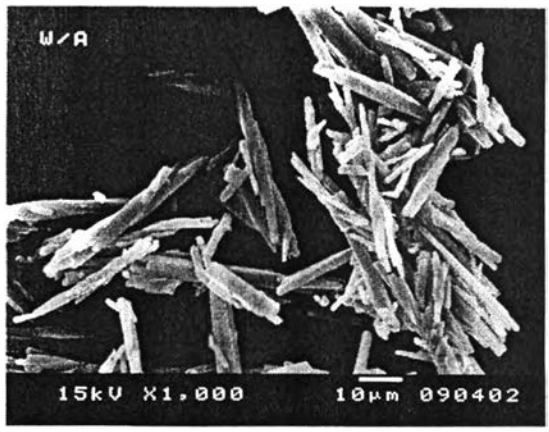

Figure 28: SEM (1000x) of VPU crystal recrystallized from Ethanol/water by method IV

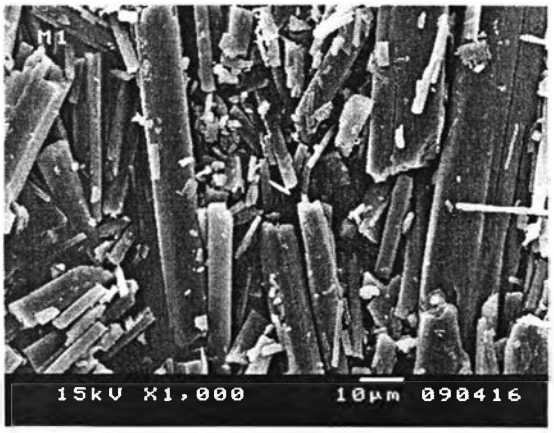

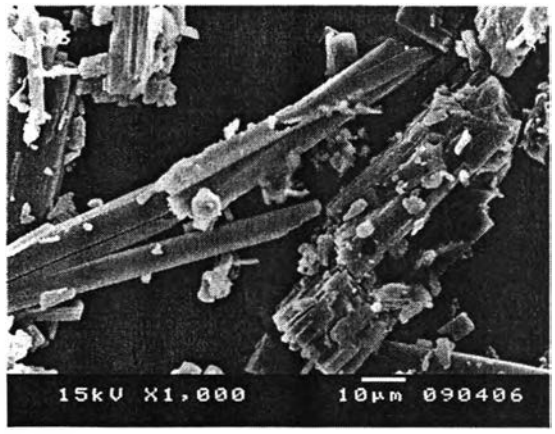

Figure 29: SEM (1000x) of VPU crystal obtained from evaporation recrystallization (Method V)

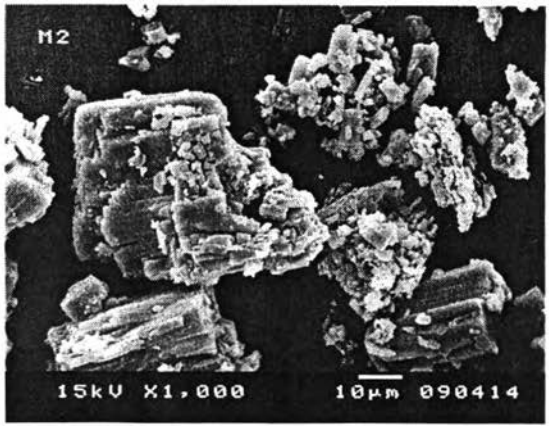

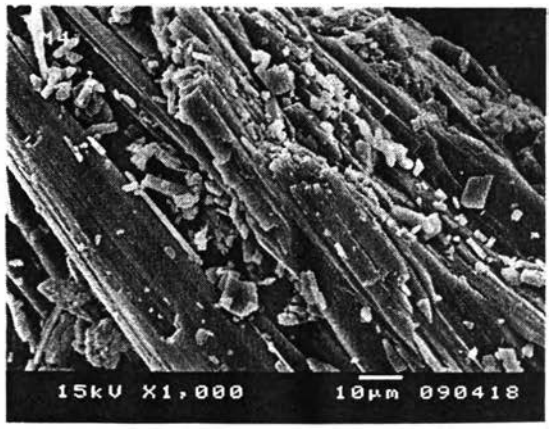

Figure 30: SEM (1000x) of VPU crystal obtained from immediate solidification of melt (Method VI)

2.2.2 X-ray Powder Diffraction analysis

Since every compound produces its own characteristic powder pattern owing to the unique crystallography of its structure, powder x-ray diffraction is clearly the most powerful and fundamental tool for a specification of the polymorphic identity of substances (51,52).

XRPD pattern of reference VPU exhibits just a small peak at the position where $2\theta = 19.2°$ (Figure 11). The products treated by method I obtained from hexane and heptane do not have this peak at all (see Figure 31), while the products obtained from benzene, diethyl ether and ethyl acetate have high intensity peak at this 2θ (see Figure 32). XRPD patterns of the products recrystallized from the rest of the solvents have peak at $2\theta = 19.2°$ smaller than the peaks of the products recrystallized from benzene, diethyl ether and ethyl acetate (see Appendix).

From the XRPD patterns, the products can be grouped as

(a) exhibit peak at $2\theta = 19.2°$ (representative of this group was the product obtained by recrystallized from diethyl ether and benzene) and;

(b) absent of peak at $2\theta = 19.2°$ (representative of this group was the product obtained by recrystallized from heptane and heptane).

This result indicated that solid state transformation of VPU may exist when recrystallized in various solvents.

Further investigation by DSC and TGA were used to confirm this result. There were no differences between the DSC/TGA thermograms obtained from reference VPU (Figure 13) and the products recrystallized from heptane and diethyl ether by method I (Figure 33,34).

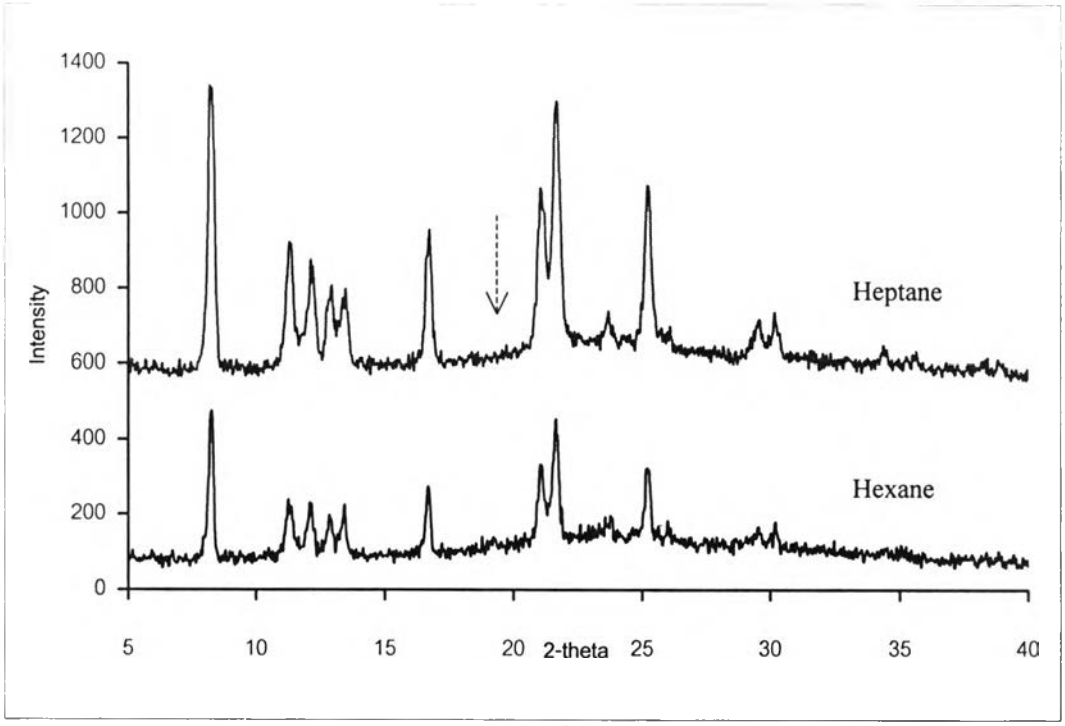

Figure 31: XRPD patterns of the products recrystallized from hexane and heptane by method I

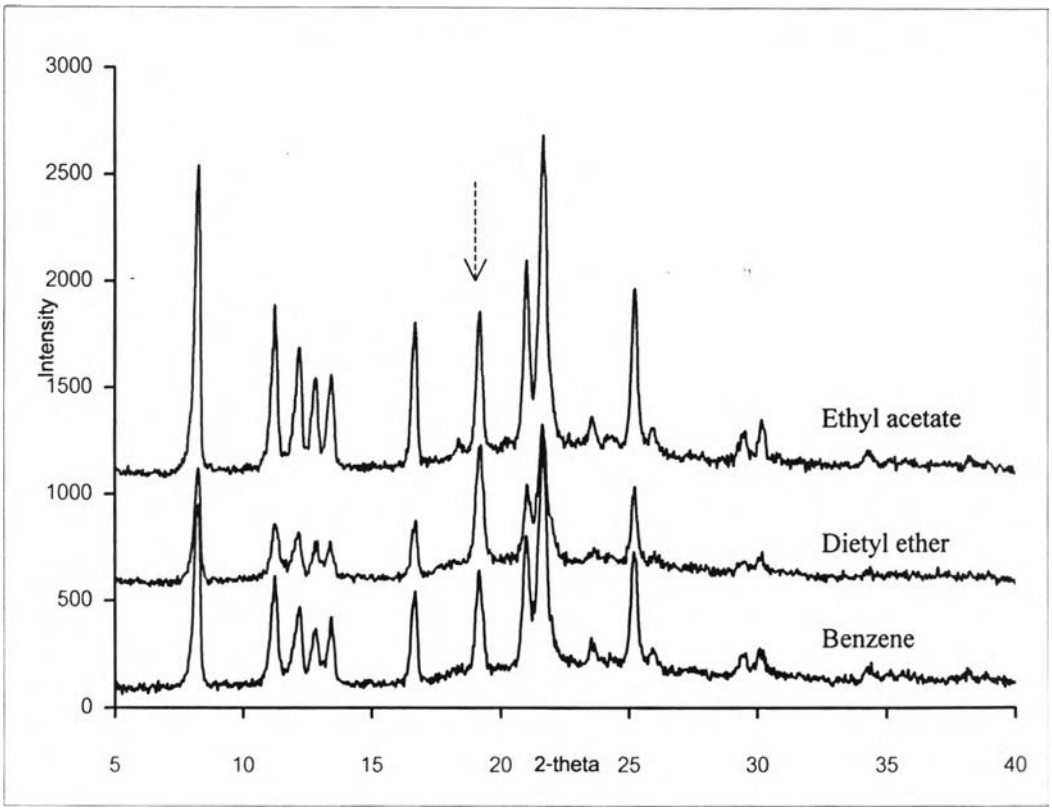

Figure 32: XRPD patterns of the products recrystallized from benzene, diethyl ether and ethyl acetate by method I

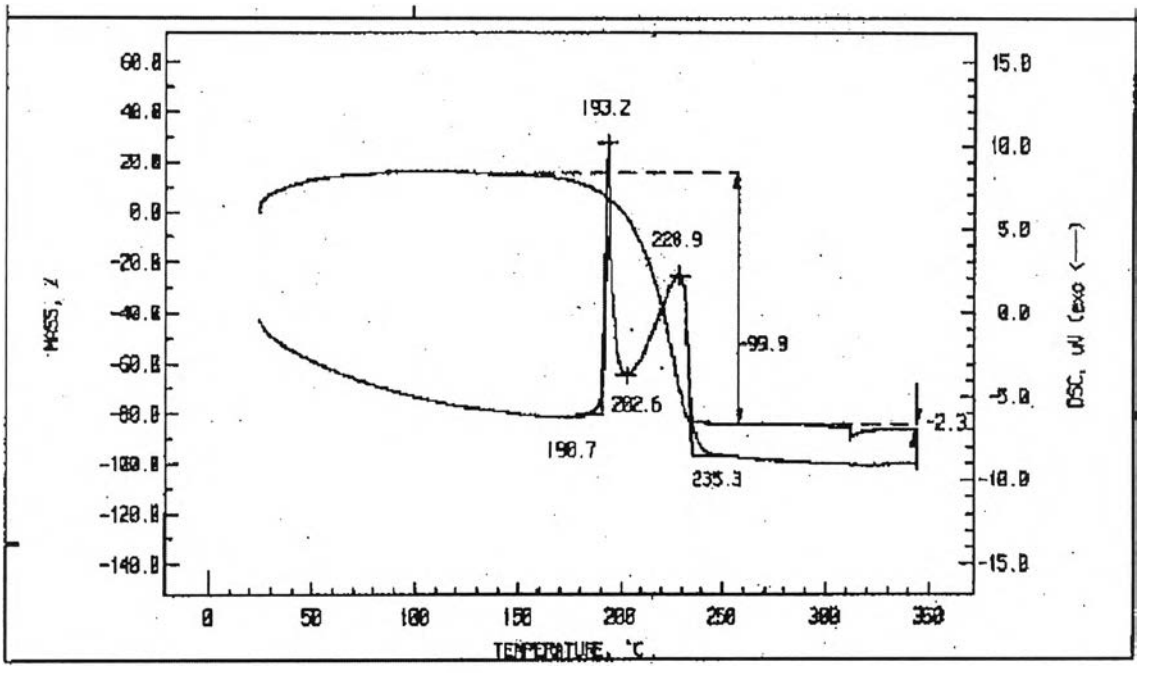

Figure 33: DSC/TGA thermogram (15°C/min) of the product obtained from heptane by method I

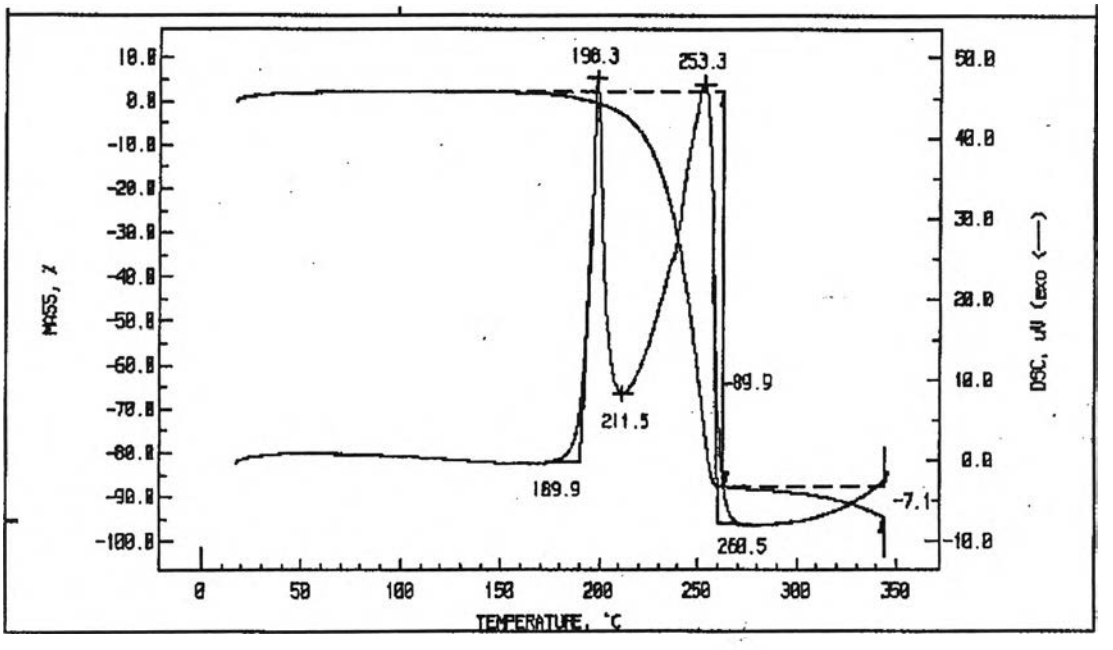

Figure 34: DSC/TGA thermogram (15°C/min) of the product obtained from diethyl ether by method I

Since only single peak at $2\theta = 19.2°$ is different between these two groups, the difference should not be the result of preferred orientation but may occurred from internal structure variation. However, possibly this minor internal structure variation may have little effect on thermoanalytical behavior of the product because the difference in DSC thermograms between these two groups was not observed. These results are not conclusive and should not implied that polymorph does not exist. The single crystal XRPD analysis is required to confirm the internal structure of these molecules.

Since these results can not confirm polymorph existence, rescreening must be conducted. In rescreening studies, the products obtained from benzene and diethyl ether will be selected to represent group (a), while the products obtained from hexane and heptane will be selected to represent group (b). Benzene, hexane and heptane were used in method II, whereas diethyl ether was used in method III. Because crystals obtained from hexane and heptane are long needle-like form, grinding is needed before XRPD analysis. XRPD patterns of dried products recrystallized from these four solvents by the methods described all exhibited peak at $2\theta = 19.2°$ (Figure 35). Repeated study of the product obtained by hexane and heptane showed the same result indicated that no polymorph was obtainable. These products showed the same DSC thermograms compared to reference VPU mentioned in the next section. Due to the fact that the methods used were different than the first study, i.e. method I for recrystallize in hexane and heptane, the results are still inconclusive.

Attempts were made to evaluate if there were any hydrate or solvate forms by method II. This time the product was collected as a damp mass instead of dried crystals. The XRPD patterns of the damp mass obtained from hexane, heptane and benzene are similar to those of dry form with peak at $2\theta = 19.2°$ (see appendix).

The FTIR patterns of the damp mass obtained from hexane, heptane, benzene and water did not change from the reference VPU's inclined that no solvent molecule was incorporated in the crystal lattice. This result was confirmed by DSC analysis comparing the damp mass and the dry form mentioned in the next section.

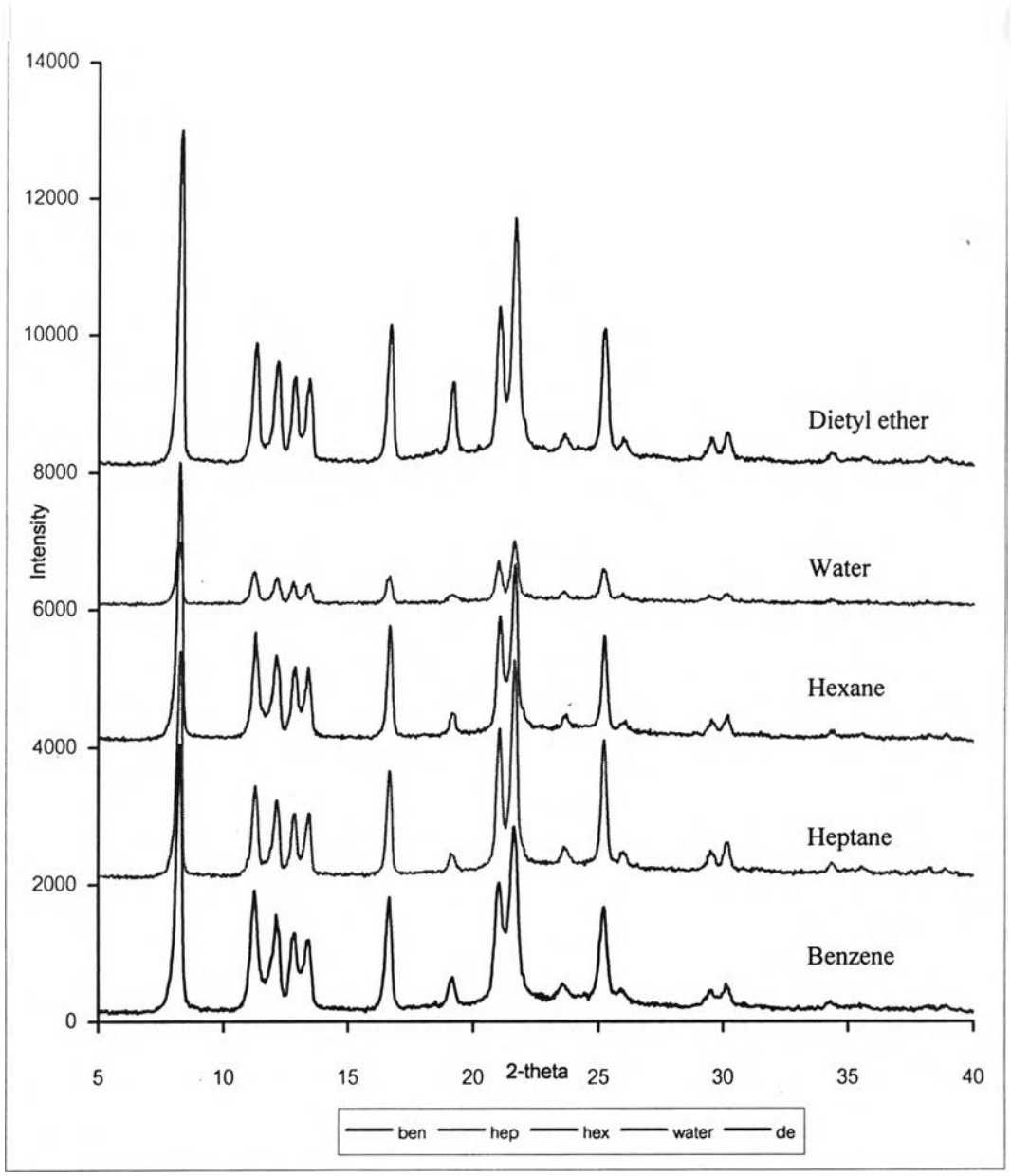

Figure 35: XRPD patterns VPU recrystallized from benzene, heptane, hexane and water by method II and recrystallized from diethyl ether by method III

In an attempt to obtain amorphous forms of VPU, the reference VPU is treated by precipitation in mixed solvent of water and methanol (method IV), evaporation crystallization (method V) and immediate solidification from melt (method VI). There are no differences in XRPD patterns among products obtained from each method and the reference VPU. Pure amorphous form of VPU could not be achieved from these methods. This finding may be the result of rapidly recrystallization of the melt of VPU during the process.

The thermal treatment method presents no polymorph transformation confirmed by XRPD analysis. However, the XRPD pattern of products exhibited some diffused pattern between 15-25° 2θ designating a decrease in degree of crystallinity of the product compared with the untreated sample (Figures 36 and 37). According to Ryan (55), relative degree of crystallinity (RDC) is calculated by using the ratio of peak intensity of treated and untreated samples as following.

$$RDC = \frac{I_{treated}}{I_{untreated}}$$

where $I_{treated}$ = peak intensity at 8.4° 2θ of treated sample;

$I_{untreated}$ = peak intensity at 8.4° 2θ of untreated sample

The peak at 8.4° 2θ was selected for this calculation because it is a single peak which exhibit the highest intensity and not affected by diffused pattern (Figure 11).

%RDC of treated product obtained from benzene = 76.69 %

%RDC of treated product obtained from heptane = 47.16 %

These values are not the true degree of crystallinity because the untreated product (reference standard) may not be 100% crystalline. Hence, the reduction of crystalline phase in the products obtained from both solvents are different due to both untreated products may have different degree of crystallinity. Moreover, the reference standards selected will also influence the numerical value of the percent crystallinity in the first place. Therefore, the degree of crystallinity values obtained using one set of standards and a particular experimental method may not agree with values obtained using other standards or another experimental method (51).

The result suggests that VPU crystals may be transformed to an amorphous form during heating process. This finding is sufficiently attractive for further study, because heating process is one of the most important processes in production of dosage form. Moreover, amorphous form exhibited distinctive properties from crystalline form and usually has higher solubility compared with the more stable crystalline form. Future study in solid state stability will emphasize on the rate of solid state transformation from crystalline VPU to amorphous form.

DSC thermogram of the thermal treated product did not show a difference in the pattern when compared with reference VPU.

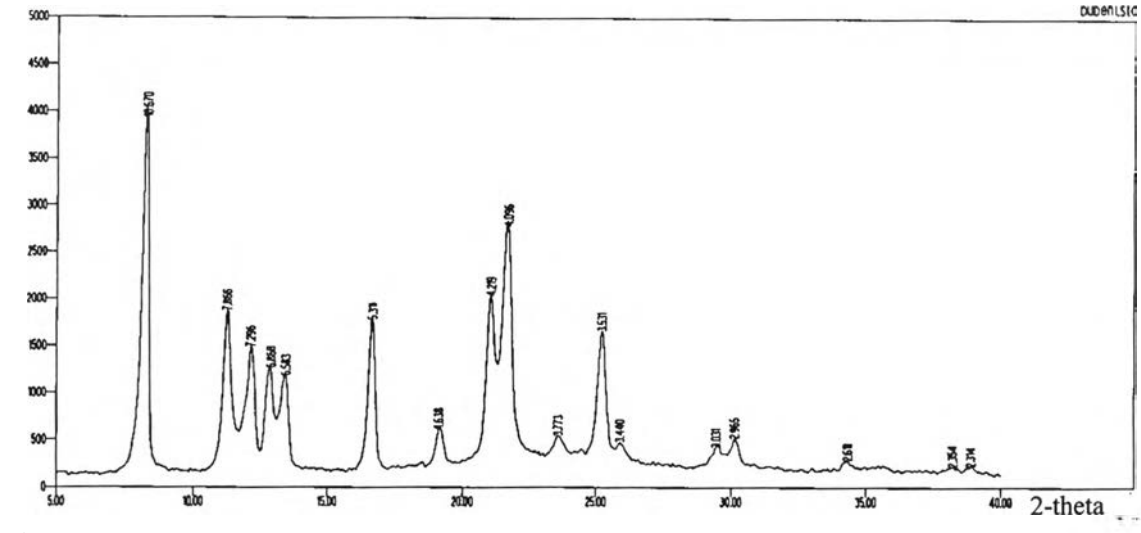

a)

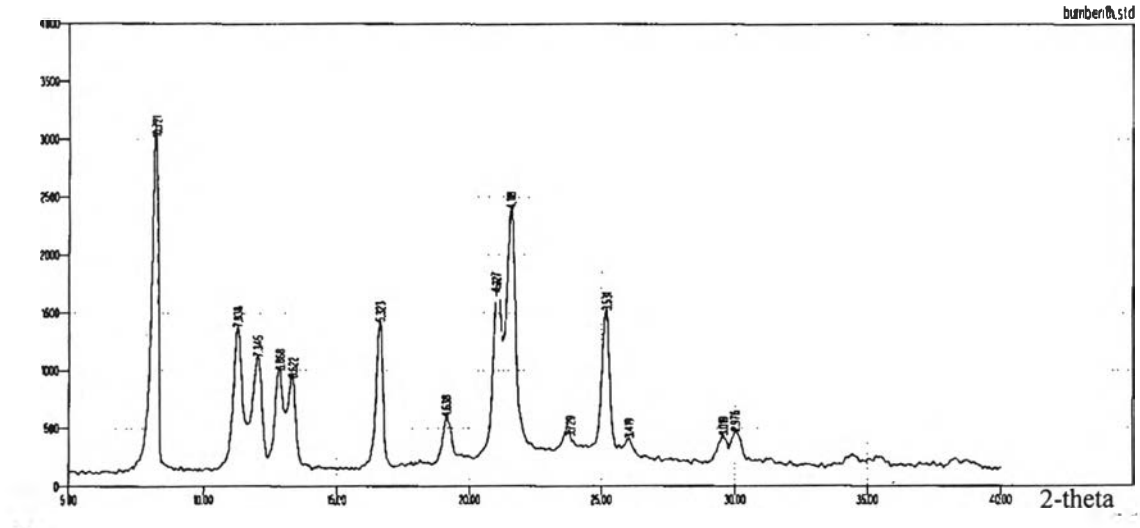

b)

Figure 36: XRPD patterns of VPU obtained from benzene by method II: a) before thermal treatment; b) after thermal treatment

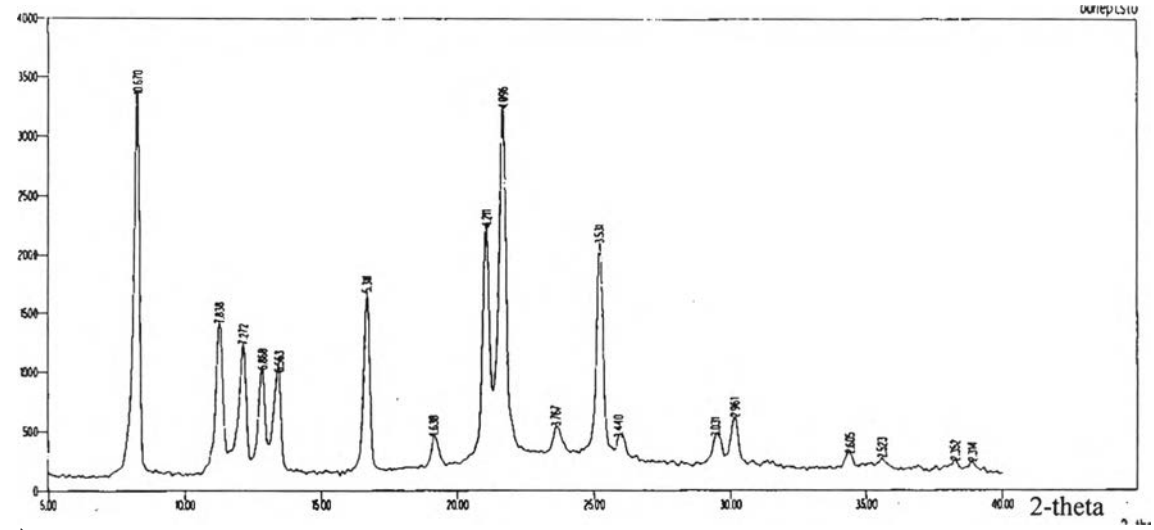

a)

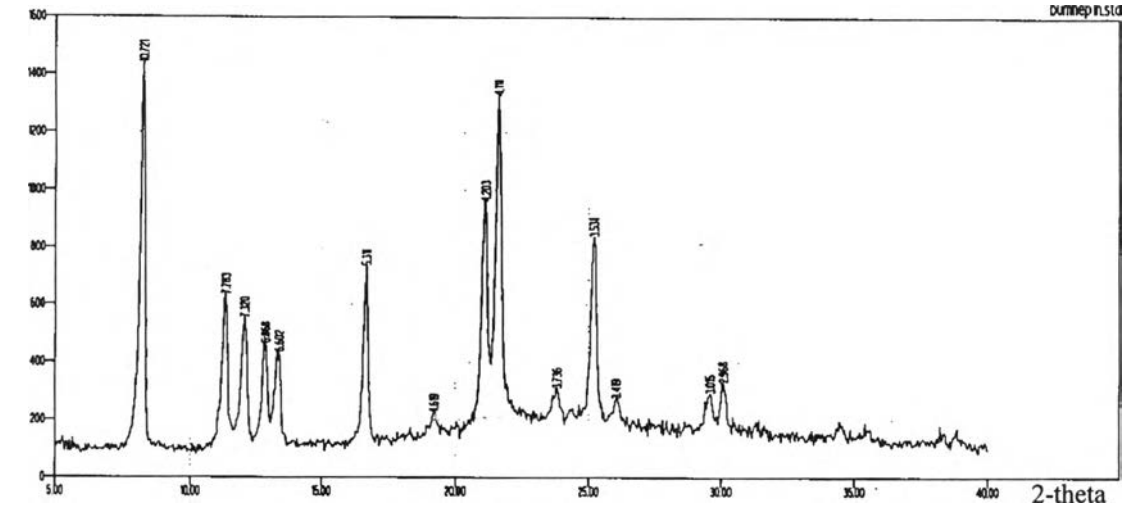

b)

Figure 37: XRPD patterns of VPU obtained from heptane by method II: a) before thermal treatment; b) after thermal treatment

2.2.3 Thermogravimetric and Differential Scanning Calorimetry Analysis

There are no differences among TGA/DSC curves obtained from VPU recrystallized from heptane and diethyl ether by method I (Figures 33 and 34) and reference VPU (Figure 13), as was discussed in the XRPD section.

Rescreening products obtain from benzene, hexane and heptane by method II and that obtained from diethyl ether by method III present similar DSC thermograms (Figure 38-41), which were not different from DSC thermogram of reference VPU.

DSC/TGA thermogram obtained from the product recrystallized from water by method II (Figure 42) is not different from that of the reference VPU (Figure 13). DSC thermograms of dry forms VPU products obtained from hexane, heptane and water by method II (see appendix) are not different from DSC thermogram of the reference VPU (Figure 12). Although DSC thermograms of damp mass VPU products obtained from hexane, heptane, benzene and water by method II present endothermic peak at each solvent boiling points, but XRPD showed otherwise due to the fact that DSC analysis was conducted with moist product (see Appendix B). Using the results of both XRPD and DSC confirmed that no solvent molecule was incorporated in the crystal lattice, thus no solvate or hydrate forms exist.

DSC thermograms of VPU products obtained from recrystallized in mixed solvent (method IV), from evaporation crystallization (method V), from immediate solidification of the melt (method VI) and from thermal treatment (method VII) are also similar to DSC thermograms of the reference VPU (see Appendix B).

The results obtained from XRPD, DSC and TGA analysis may imply that VPU treated by all methods used in this investigation (except recrystallization from hexane and heptane by method I) did not possess any polymorph, solvate or hydrate transformation. These may be the result of an intramolecular and intermolecular hydrogen-bonding of VPU (5). The intramolecular and intermolecular hydrogen-bonding may restrict the conformation of VPU and in turn affect the crystalline structure of VPU.

According to the study by Wicharn Janwitayanuchit (5), VPU has a possibility to form intramolecular hydrogen bonding suggested by its NMR pattern. Figure 43 showed proposed intramolecular hydrogen bonded structure of this compound, the intramolecular hydrogen bonded form built a stabilized six membered ring structure of the compound. In addition, VPU may also exhibit characteristic extent of intermolecular hydrogen bonding.

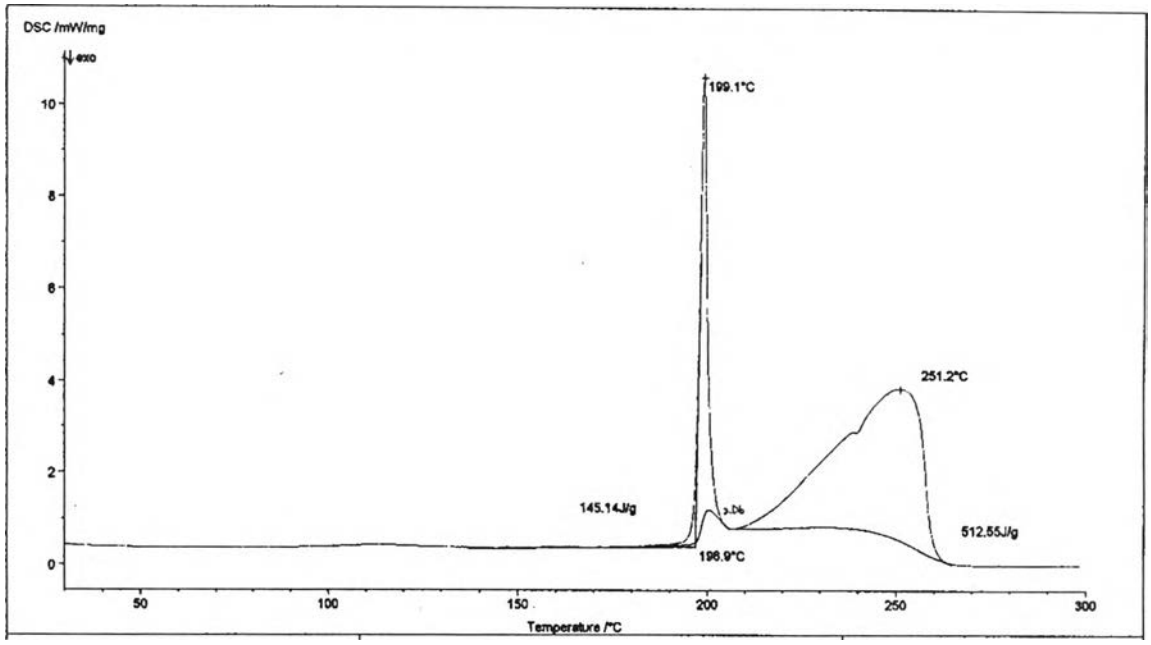

Figure 38: DSC thermogram (10°C/min) of the product obtained from benzene by method II

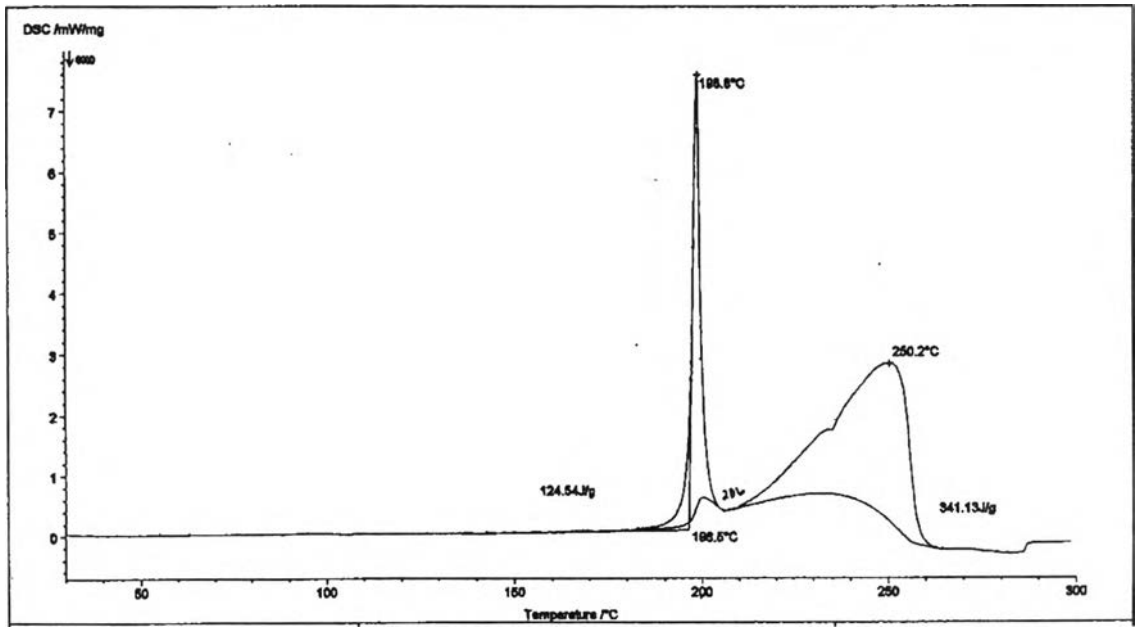

Figure 39: DSC thermogram (10°C/min) of the product obtained from heptane by method II

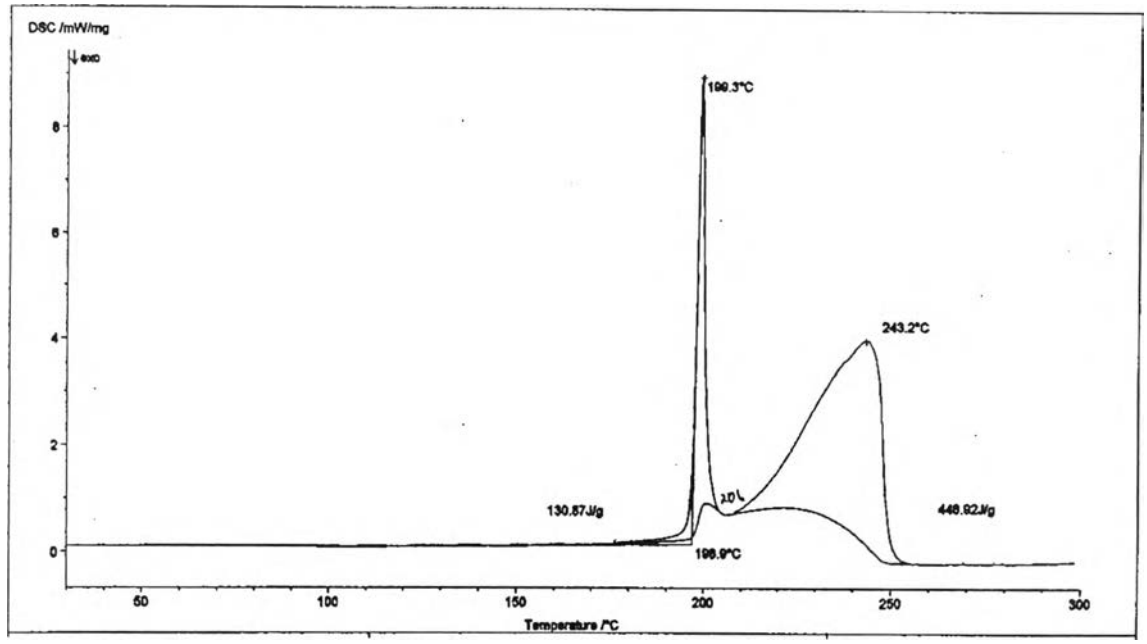

Figure 40: DSC thermogram (10°C/min) of the product obtained from hexane by method II

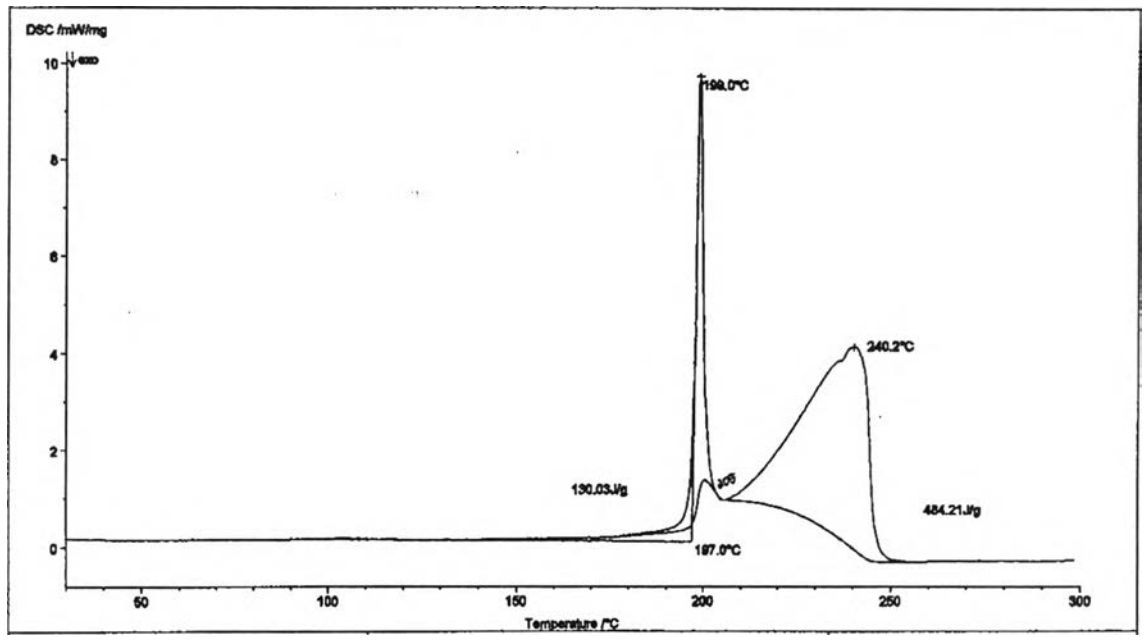

Figure 41: DSC thermogram (10°C/min) of the product obtained from diethyl ether by method II

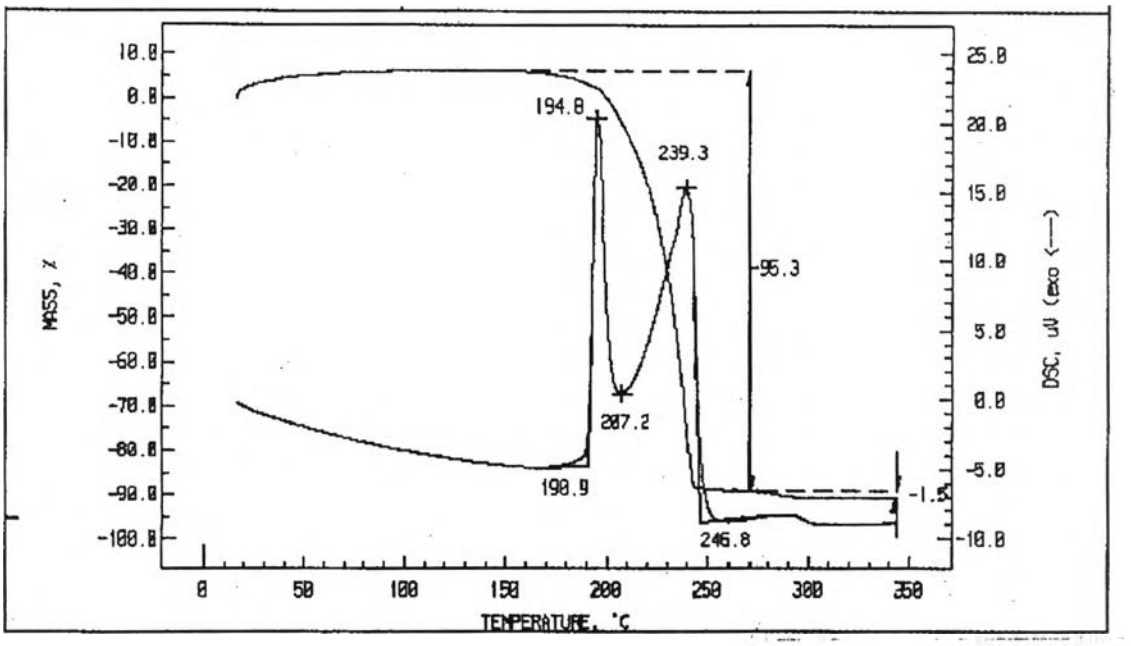

Figure 42: DSC/TGA thermogram (15°C/min) of the product obtained from water by method II

8.39

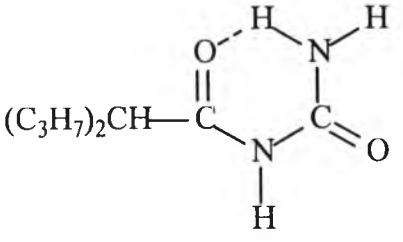

5.48

9.20

Figure 43: Proposed structure of VPU showing intramolecular hydrogen bonding

III Solid State Stability

Solid state reaction can be categorized either as a chemical reaction or as physical transformation (37). The physicochemical transformations such as polymorphic transitions, solvations and desolvations affects the pharmaceutically important physical properties such as solubility, flow and tableting behavior (12-14). The objective of this investigation was to examine solid phase transformation of VPU over a range of temperatures as a function of time.

Solid phase screening by thermal treatment method suggested that the reference VPU could gradually change from crystalline structure to a mixture of crystalline and amorphous phase. This finding is indicated by a reduction in the degree of crystallinity (55).

The morphology of samples collected at 4 weeks interval shown in Figure 44 demonstrated that at higher temperature, increasing number of small particles occurred on the surface of the crystals. This finding suggested that, the higher temperature used in the study, the more crystal breakage occurred. This may resulted from the disorder of arrangements of molecules at high temperature, which decrease the degree of crystallinity. This finding was confirmed by XRPD analysis that more amorphous phase was present (14,20).

The TLC and FTIR patterns obtained from all samples are identical to that of reference VPU suggested that the samples have the same chemical identity with the reference VPU.

From the assumption that the transformation must be greatest at 80°C, hence, DSC must be conducted with the sample placed at 80°C for 4 weeks. DSC thermogram of sample obtained from stability study at 80°C for four weeks is similar to that of reference VPU (see appendix B).

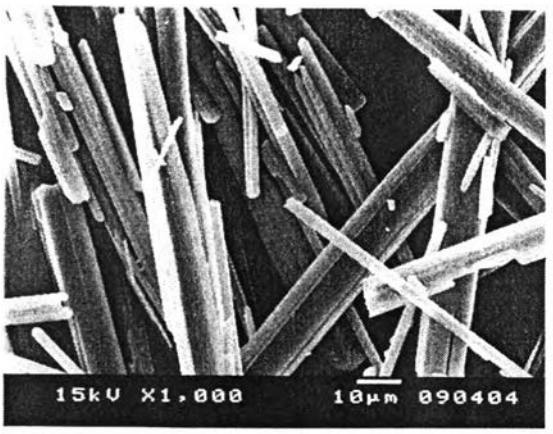

a) 50°C

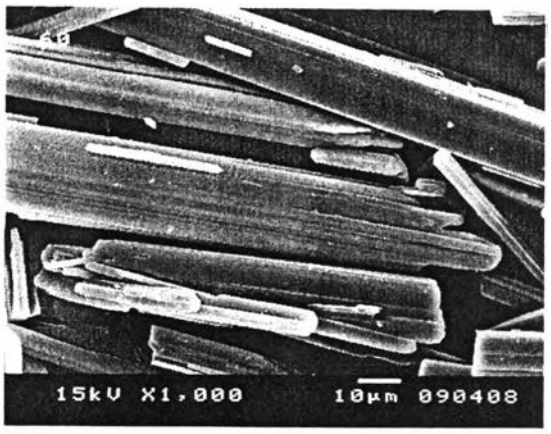

b) 60°C

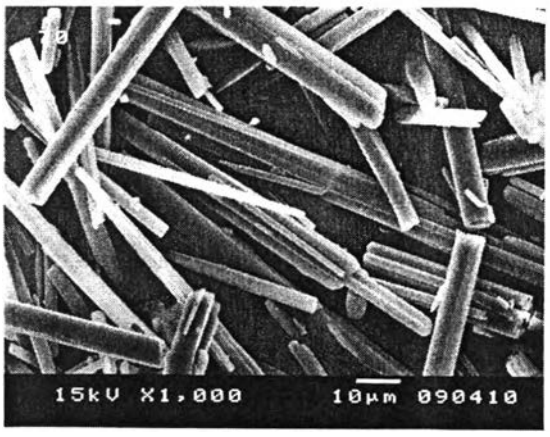

c) 70°C

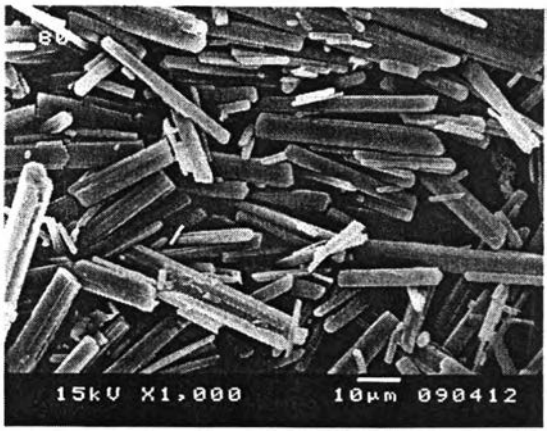

d) 80°C

Figure 44: SEM photomicrographs of the samples obtained from solid state stability study for four weeks, a) 50°C, b) 60°C, c) 70°C, d) 80°C

The accelerated thermal stability study of VPU was performed to investigate the effect of temperature on structural change using XRPD analysis. Quantitative XRPD analysis was conducted using continuous scan from 5-40° 2θ, using sodium chloride as an internal standard.

Quantitative XRPD analysis using an internal standard was described in detail by Suranarayanan (52, 53). Klug and Alexander (53) derived a general equation for a mixture consisting several solid components. This mixture, however, can be regarded as being composed of just two main components: component J (which is the unknown), and the sum of the other components (which is designated as the matrix). Following the addition of an internal standard (component S) to the sample in known amount, the integrated XRPD intensities of line i of component J, I_{iJ}, and line k of component, S, I_{kS}, are determined. The weight fraction of the unknown component is the original sample, x_J, is given as

$$x_J = KI_{iJ}/I_{kS}$$

where K is a constant. When the internal standard is added in a constant proportion, the concentration of component J is a linear function of the intensity ratio, I_{iJ}/I_{kS}.

The system in this study composed of two components; crystalline phase of VPU, which is assigned as the unknown, and the amorphous phase as matrix.

Attempts were made to quantitate the absolute amount of crystalline phase of VPU by constructing calibration curved from a physical mixture of crystalline and pure amorphous solids. According to solid phase screening, the pure amorphous VPU was not obtainable either by rapid evaporation from several solvents (Method I), precipitation by addition of sparingly soluble solvent (Method III), immediate solidification of the melt or by high temperature treatment. Thus, it was not possible to construct the calibration curve.

Instead the intensity ratio of I_{VPU}/I_{NaCl} will be used to represent as relative amount of crystalline VPU in mixture. Since variation in lattice strain and particle size can have significant influence on the line shape, but these will not affect the integrated intensity (area under the curve). Hence, the integrated intensity or area under the curve should be used in the calculation instead of just peak intensities (52).

The diffraction peak of VPU at a 2θ value of 8.4° was selected for measurement because it is a single peak, which exhibited the highest intensity, thus it is suitable to use this peak in quantitative analysis (Figure 45). Moreover, this peak was not affected by disorder of XRPD pattern (amorphous halo) due to the present of amorphous phase. Indicated by XRPD pattern obtained by thermal treatment which amorphous halo occurred at approximately 2θ value of 15-25° (Figure 36, 37).

Sodium chloride was chosen as the internal standard because the 2θ value of its highest intensity peak appeared at 2θ value of approximately 31.7°C did not interfere with the XRPD pattern of VPU (Figure 45).

A preliminary study done by varying concentration of sodium chloride at 5, 10, 20, 30 and 40% w/w indicated that 10% concentration was most appropriate because the highest intensity value of sodium chloride was similar to that of VPU (Figure 46).

The relative amount of crystalline phase of VPU in the samples was calculated as the intensity ratio of I_{VPU}/I_{NaCl} as follows:

$$X_{rc} = \frac{I_c}{I_{NaCl}}$$

where x_{rc} = relative amount of crystalline phase of VPU

I_c = Integrated intensity of VPU at 2θ = 8.4°

I_{NaCl} = Integrated intensity of sodium chloride at 2θ = 31.7°

The samples collected at a definite time interval of 2 weeks and 4 weeks were added with 10% w/w sodium chloride and then determined the integrated intensity of the peak at 2θ = 8.4° and 31.7°. The intensity ratio is the average of three determinations shown in table 5.

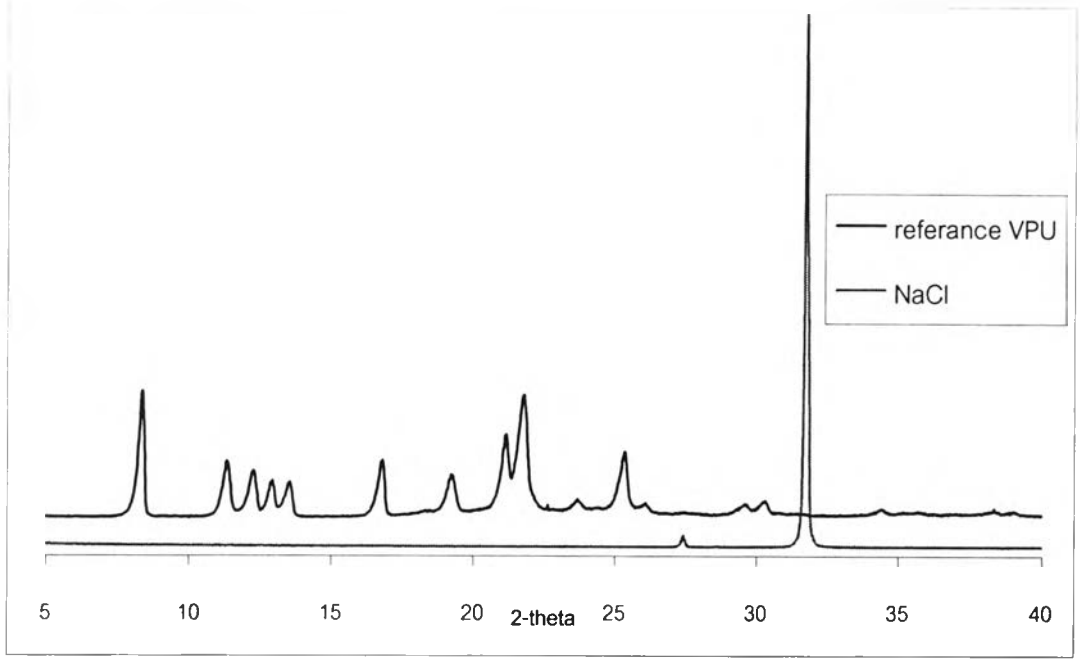

Figure 45: XRPD patterns of reference VPU and sodium chloride

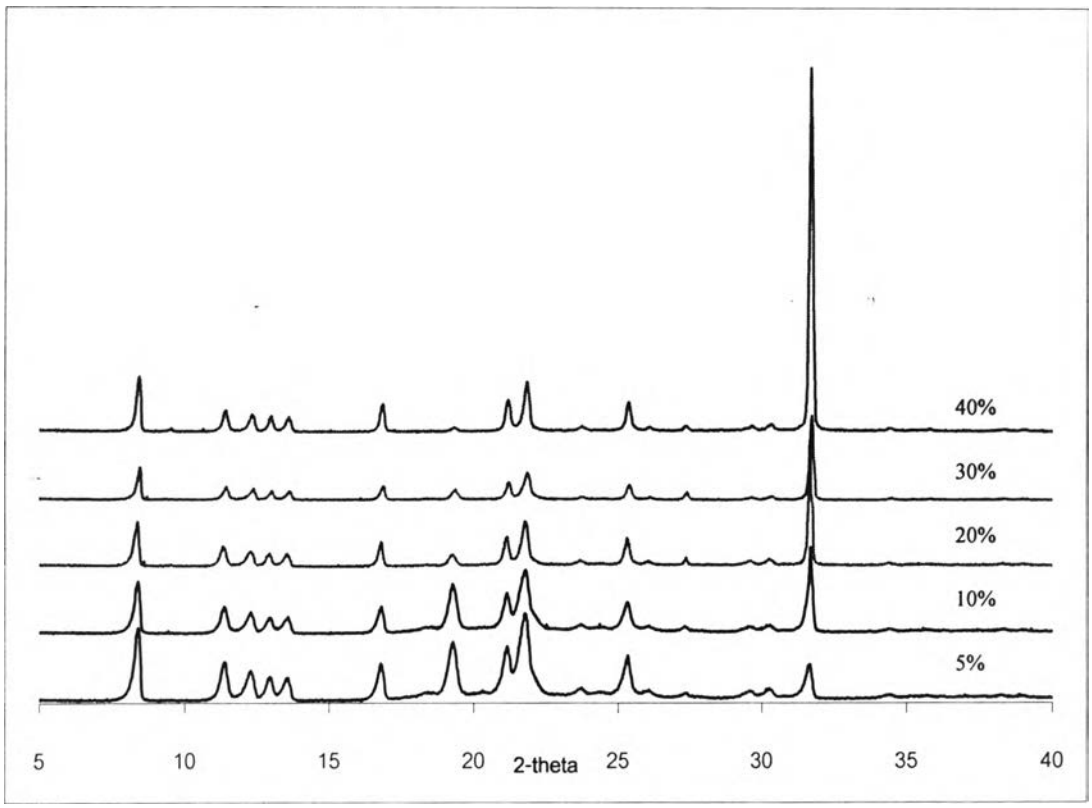

Figure 46: XRPD patterns of the reference VPU mixed with
5%, 10%, 20%, 30% and 40% of sodium choride

Table 5: Integrated intensity ratio of VPU and sodium chloride of the samples obtained from stability study

Time (weeks) / Temp. (°C)	0		2		4	
	Average intensity ratio	Standard deviation	Average intensity ratio	Standard deviation	Average intensity ratio	Standard deviation
50	1.0661	1.4360×10^{-1}	1.0484	5.5600×10^{-2}	1.0428	7.9700×10^{-2}
60			1.0107	4.0550×10^{-1}	9.4780×10^{-1}	9.5700×10^{-2}
70			8.9260×10^{-1}	1.8410×10^{-1}	8.4750×10^{-1}	2.1500×10^{-2}
80			8.5240×10^{-1}	4.2600×10^{-2}	7.5790×10^{-1}	4.2100×10^{-2}

To investigate the kinetics of transformation, a plot of relative amount of crystalline phase of VPU x_{rc}, versus time t, using correlated equation was produced. From preliminary study, solid VPU has transformed from crystal form to amorphous form. The equations that may relate to this transformation are the kinetic equations based on reaction orders and the reactions controlled by contracting geometries that occurred from progression of phase boundaries from the outside to the inside of the crystal. The reaction control by nucleation may not be concerned because of no polymorph change. Reactions controlled by diffusion are also considered to be unrelated due to no existence of solvate or hydrate form. Thus, the diffusion process was unlikely. The kinetic equations of those in concern with the transformation are shown in table 6.

Table 6: Kinetic equations used in the stability study

Equation	Reaction
$1-\alpha = kt$	Zero-order reaction
$\ln(\alpha) = kt$	First-order reaction
$1-\alpha = kt$	One Dimensional Growth of a Phase Boundary (same as Zero-order)
$1-(1-\alpha)^{1/2} = kt$	Two Dimensional Growth of a Phase Boundary
$1-(1-\alpha)^{1/3} = kt$	Three Dimensional Growth of a Phase Boundary

Where α = fraction decomposed (amorphous phase)

$(1-\alpha)$ = fraction remaining (crystalline phase)

In this study, crystalline phase was assigned as the remaining phase, but absolute amount of crystalline phase was unobtainable. Therefore, relative amount of crystalline phase ($x_{rc} = I_C/I_{NaCl}$) was used instead.

The plot of I_C/I_{NaCl} as a function of time using the equations described in the table is demonstrated as a zero-order plot (Figure 47), a first-order plot (Figure 48), a two dimensional phase boundary plot (Figure 49) and a three dimensional phase boundary plot (Figure 50).

This study conducted at two time intervals. Thus, for any equation plots compose of three points per temperature (time at 0, 2, 4 weeks interval). It is not statistically and theoretically justifies using only just few data points estimating terminal slope. Because of limited time, funds and amount of VPU, the equations have to be fitted with only these three points.

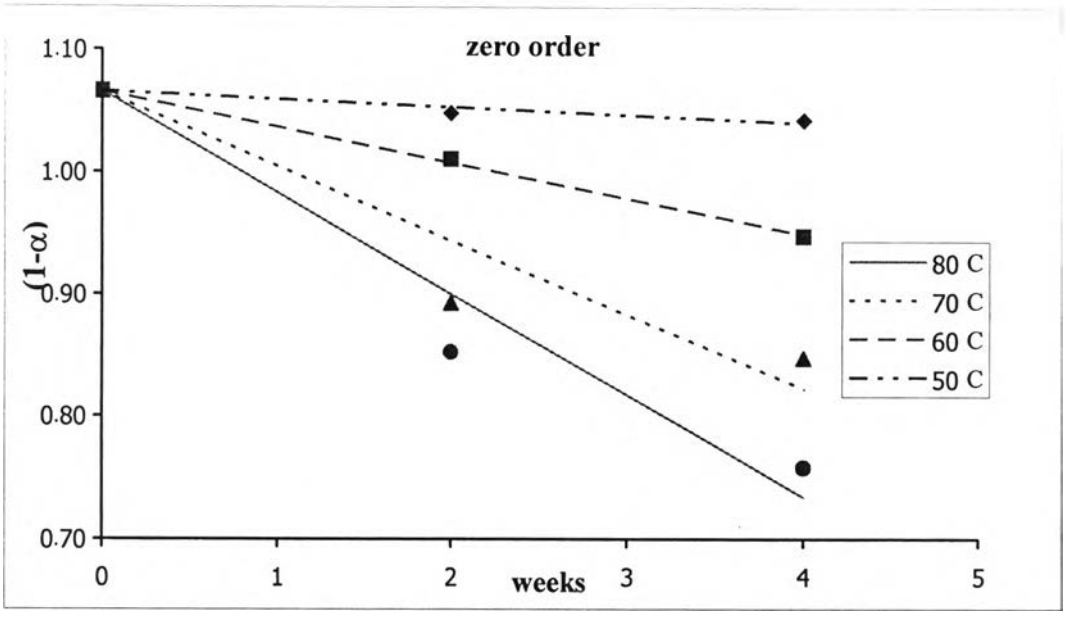

Figure 47: A plot of (1-α) versus time (Zero-order)

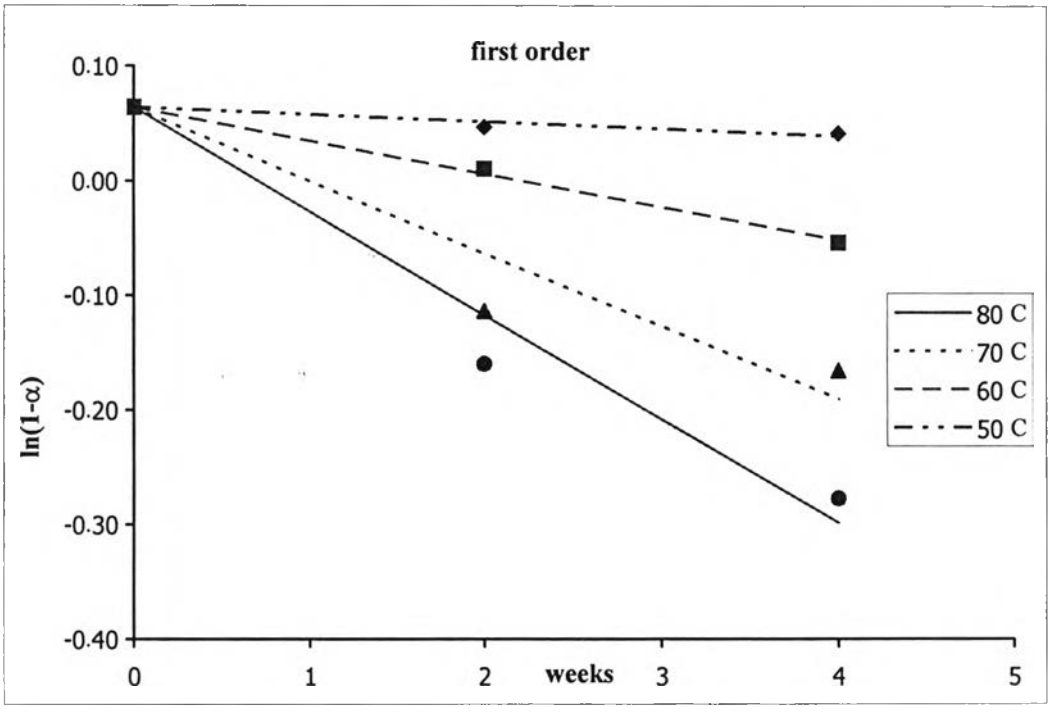

Figure 48: A plot of ln(1-α) versus time (First-order)

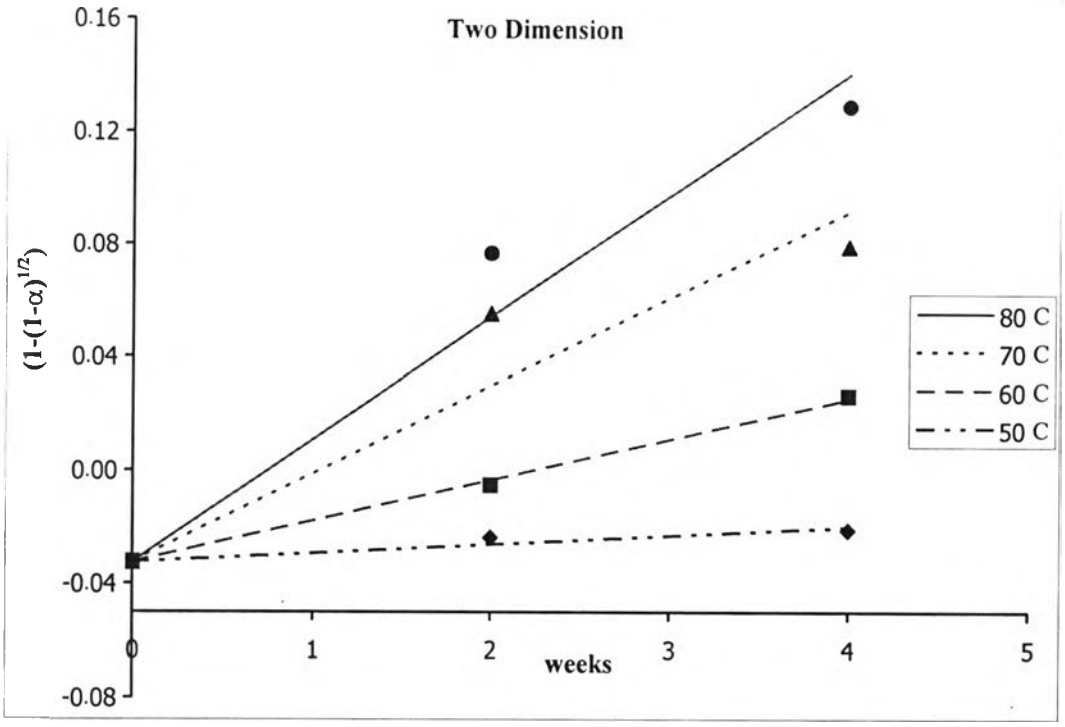

Figure 49: A plot of $(1-(1-\alpha)^{1/2})$ versus time (Two Dimensional Phase Boundary)

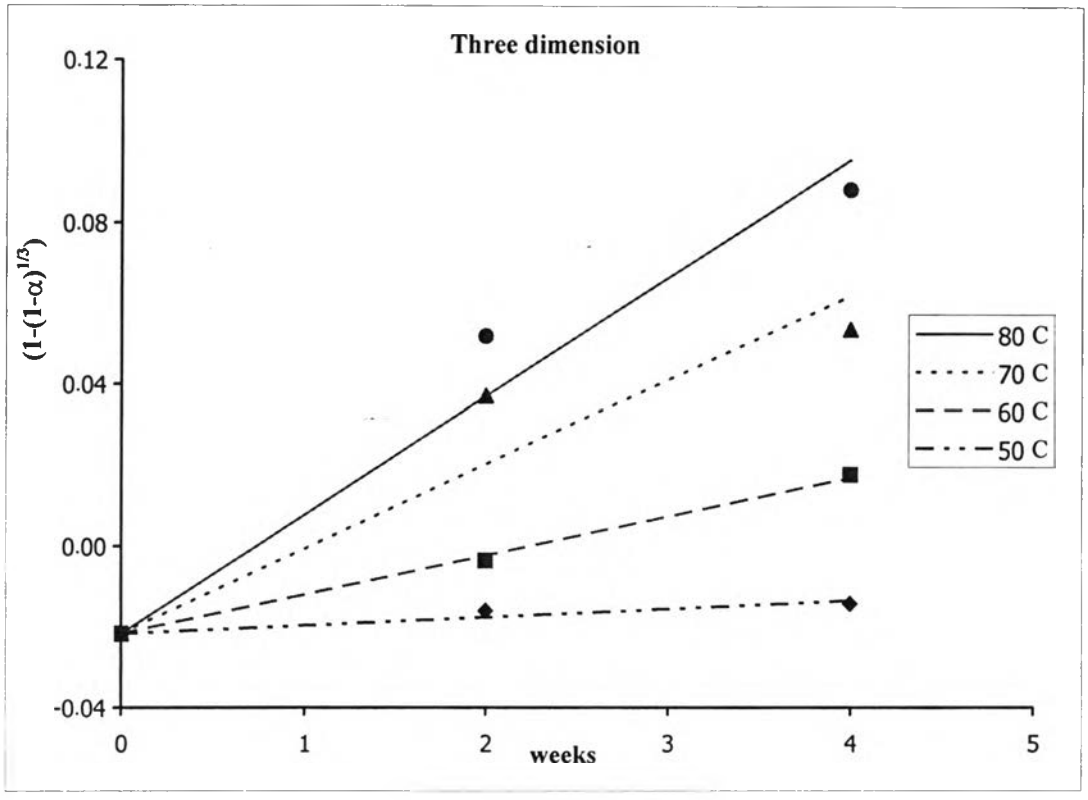

Figure 50: A plot of $(1-(1-\alpha)^{1/3})$ versus time (Three Dimensional Phase Boundary)

To determine which kinetic equations can be best fitted, the correlation of determination (r^2) is used. The correlation of determination of the four equations was examined using statistical test by Analysis of Variance (ANOVA). The results indicates that there were no significant difference among the four equations (p value < 0.05). The rate constants and the correlation of determination obtained from each reaction shown in table 7.

Table 7: The rate constants and the correlation of determination of all four kinetic equations obtained from stability study.

Reaction / Temp. (°C)	Zero order		First order		Two dimension		Three dimension	
	k_0	r^2	k_1	r^2	k_2	r^2	k_3	r^2
50	6.4000×10^{-3}	0.8993	6.1000×10^{-3}	0.9009	3.1000×10^{-3}	0.9007	2.1000×10^{-3}	0.9005
60	2.9200×10^{-2}	0.9984	2.8900×10^{-2}	0.9965	1.4500×10^{-2}	0.9975	9.7000×10^{-3}	0.9972
70	6.1100×10^{-2}	0.8763	6.3600×10^{-2}	0.8909	3.1100×10^{-2}	0.8837	2.0900×10^{-2}	0.8860
80	8.3000×10^{-2}	0.9430	9.0600×10^{-2}	0.9624	4.3300×10^{-2}	0.9531	2.9300×10^{-2}	0.9562

As mentioned above that the equations have been fitted with only three points, the difference among them possibly may not be observed. However, Byrn (70) stated that "The fact that more than one equation fits the data indicates that solid-state kinetic data cannot be used to prove the mechanism of solid-state reaction. Nevertheless it is important for the determination of the activation energy to select the proper kinetic equation".

It is not unusual to find that several kinetic equations may give excellent fits to the data; such as different dehydration mechanisms were found for sulfaguanidine monohydrate when the data was fitted using various kinetic equations (69).

According to this statement, more than one equations used in this study were proven to fit the data but it could not totally explain the mechanism of solid state transformation of VPU. Therefore, the solid state transformation may occur by several mechanisms.

Nevertheless, rate constant obtained from all equation plots indicated that the trend for transformation is greater at higher temperature.

Using Arrhenius equation, a plot of rate constant versus 1/T (Figure 51) could be used to determine the activation energy of reaction as shown in table 8.

The effect of temperature on reaction rate is given by Arrhenius equation:

$$k = Ae^{\frac{-Ea}{RT}}$$

where k = specific reaction rate

A = Arrhenius factor

E_a = Energy of activation

R = Gas constant

T = Absolute temperature

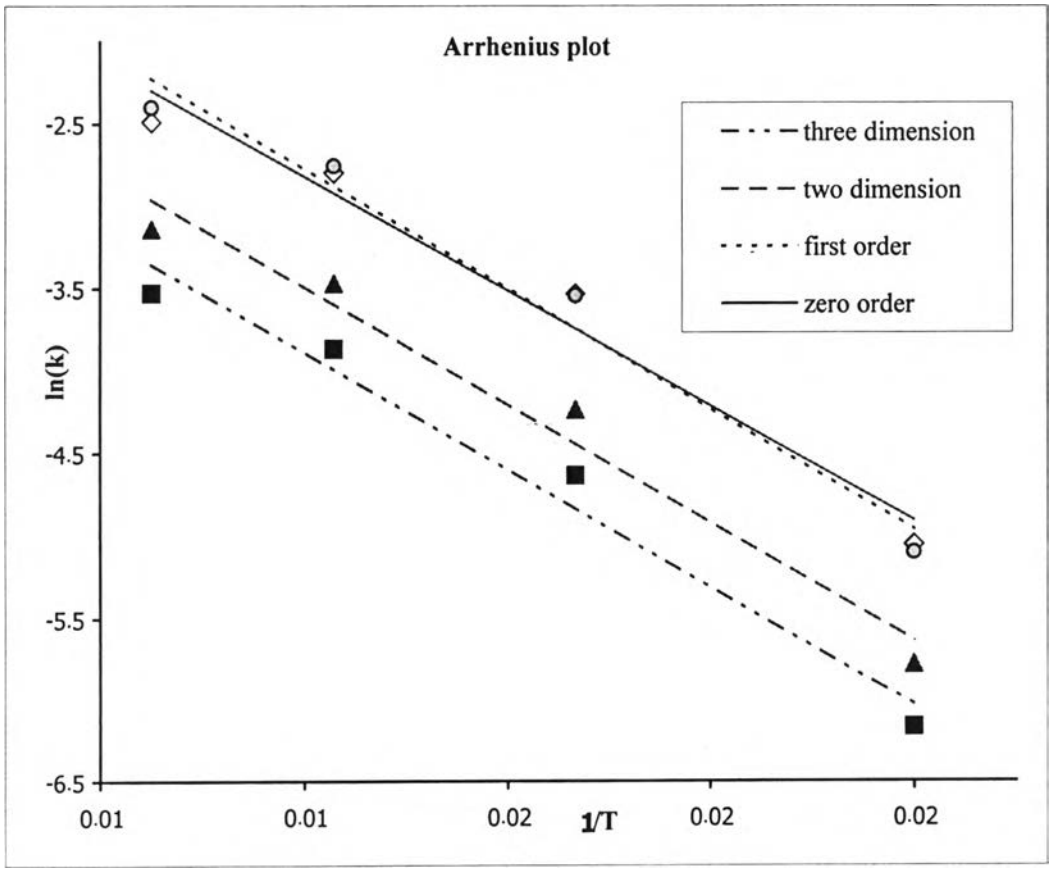

Figure 51: A plot of rate constant versus 1/T

Table 8: Activation energy of reaction obtained from correlated equations

Kinetic equations	E_a (kcal/mol.)	r^2
Zero order	174.74	0.9698
First order	183.75	0.9756
Two Dimension	179.65	0.9726
Three Dimension	179.55	0.9741

Following these results, activation energies obtained from all correlated equations was not significant different. Therefore, the major transformation pathway occurred was not obtainable.

IV SOLUBILITY MEASUREMENTS

Since VPU has a poor aqueous solubility property that may prove to be a disadvantage in the future product development. Existence of amorphous form is one of the opportunities to increase the solubility of the compound (14,16). The equilibrium solubility of reference VPU was measured and compared with the solubility of sample obtained from stability study at 80°C for four weeks due to this sample exhibited the highest transition to amorphous form. Solubility of the reference VPU and the sample is shown in Figure 52.

According to several studies reviewed and done by Hancock and Parks (16), many amorphous pharmaceuticals are markedly more soluble than their crystalline counterparts. For example aqueous solubility of amorphous indomethacin compared with its γ-crystal form was 4.5 fold. This was also true with VPU, its amorphous form presented higher solubility than the crystal form. Figure 52 showed that the sample exhibited high solubility at the early state, which may be due to amorphous phase in sample. In the later state, there is a reduction in solubility due to amorphous may recrystallized to crystal form. Final solubility of both the reference VPU and the

sample is almost similar. The sample presented the highest solubility at time = 2 hours which 1.4 times greater than that of the reference VPU (Table 9).

Brittain and Grant (76) stated that, "For a solid to dissolve, the forces of attraction between solute and solvent molecules must overcome the attractive forces holding the solid and the liquid solvent together. For the process to proceed spontaneously, the solvation free energy released upon dissolution must exceed the sum of the lattice free energy of the solid plus the free energy of cavity formation in the solvent. The balance of the attractive and disruptive forces will determine the equilibrium solubility of the solid."

Brittain and Grant (76) added that "A solid having a higher lattice free energy will tend to dissolve faster, because the release of a higher amount of stored lattice free energy will increase the solubility and hence the driving force for dissolution." The high internal energy and specific volume of the amorphous state relative to the crystalline state can lead to enhanced dissolution and bioavailability (32).

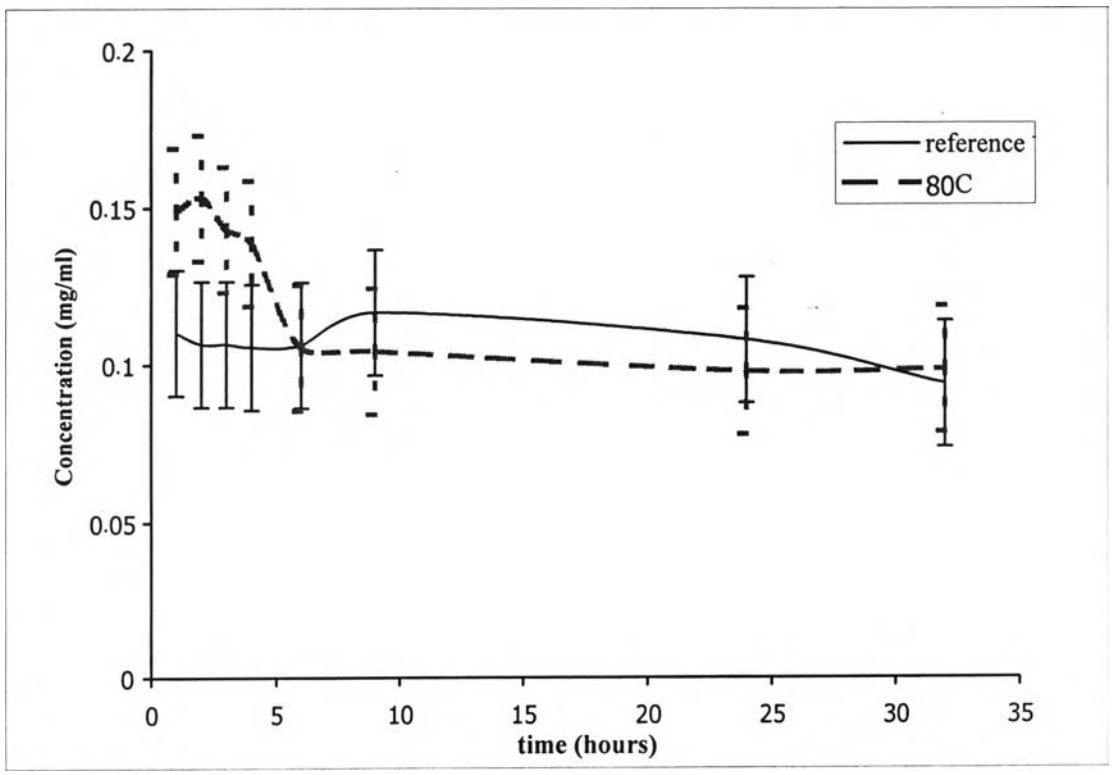

Table 9: Concentrations of the the reference VPU and the samples obtained from stability study at 80 °C for 4 weeks in several time intervals

Conc. (mg/ml) / Time (hr)	Reference VPU	Sample from 80°C, 4 weeks
1 hr	0.1103	0.1490
2 hr	0.1065	0.1532
3 hr	0.1065	0.1431
4 hr	0.1056	0.1387
6 hr	0.1062	0.1054
9 hr	0.1166	0.1043
24 hr*	0.1079	0.0979
32 hr	0.0940	0.0986